Prepared for the National Park Service

Marine Benthic Habitat Mapping of the West Arm, Glacier Bay National Park and Preserve, Alaska

By Timothy O. Hodson, Guy R. Cochrane, and Ross D. Powell

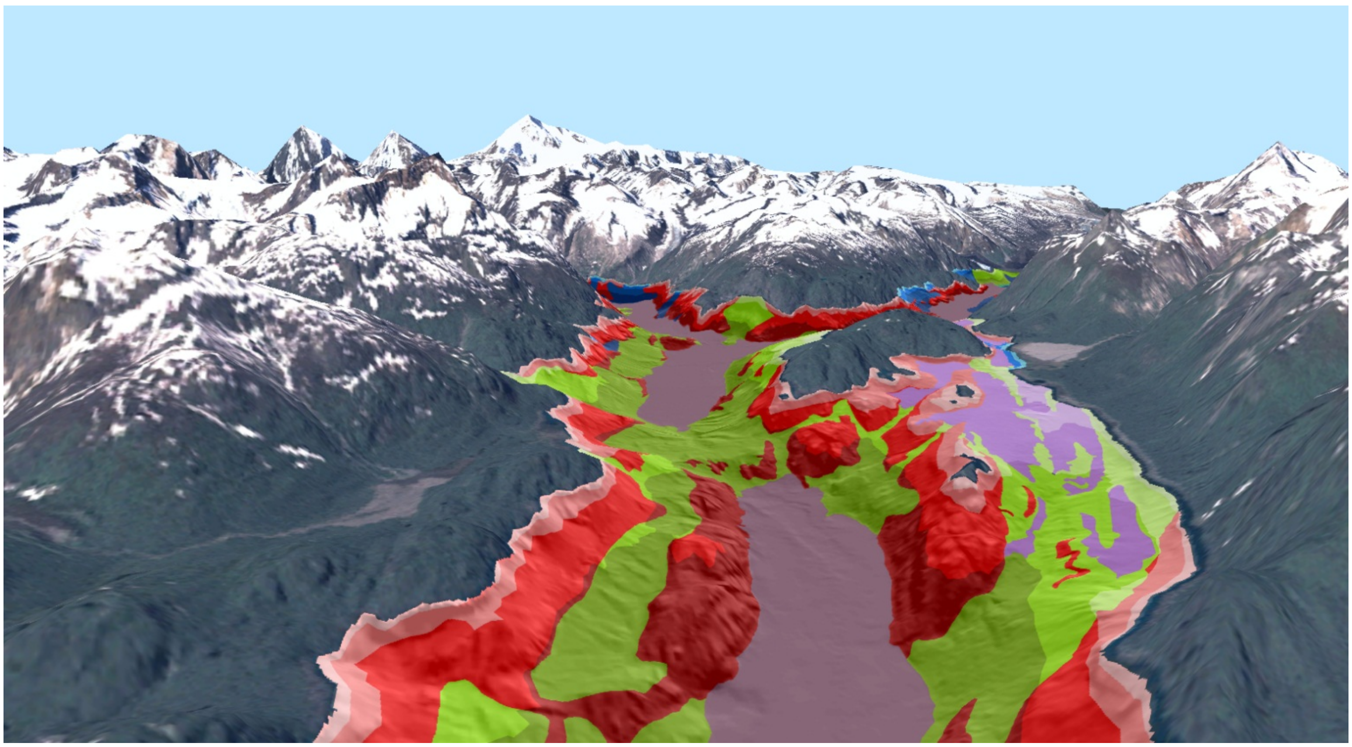

Pamphlet to accompany

Scientific Investigations Map 3253

2013

U.S. Department of the Interior
U.S. Geological Survey

Contents

Figures

Tables

Marine Benthic Habitat Mapping of the West Arm, Glacier Bay National Park and Preserve, Alaska

By Timothy O. Hodson, Guy R. Cochrane, and Ross D. Powell

Abstract

Seafloor geology and potential benthic habitats were mapped in West Arm, Glacier Bay National Park & Preserve, Alaska, using multibeam sonar, groundtruthed observations, and geological interpretations. The West Arm of Glacier Bay is a recently deglaciated fjord system under the influence of glacial and paraglacial marine processes. High glacially derived sediment and meltwater fluxes, slope instabilities, and variable bathymetry result in a highly dynamic estuarine environment and benthic ecosystem. We characterize the fjord seafloor and potential benthic habitats using the recently developed Coastal and Marine Ecological Classification Standard (CMECS) by the National Oceanic and Atmospheric Administration (NOAA) and NatureServe. Due to the high flux of glacially sourced fines, mud is the dominant substrate within the West Arm. Water-column characteristics are addressed using a combination of CTD and circulation model results. We also present sediment accumulation data derived from differential bathymetry. These data show the West Arm is divided into two contrasting environments: a dynamic upper fjord and a relatively static lower fjord. The results of these analyses serve as a test of the CMECS classification scheme and as a baseline for ongoing and future mapping efforts and correlations between seafloor substrate, benthic habitats, and glacimarine processes.

Introduction

This study is a bottom-up approach to mapping benthic habitats (see Greene and others, 2007) in the West Arm of Glacier Bay National Park & Preserve (fig. 1). Seafloor substrate and morphology are characterized so that they may be correlated to and associated with a specific set of benthic conditions favorable for local biota. These include commercially and recreationally important species such as king crabs (*Paralithodes camtschaticus*), Tanner crabs (*Chionoecetes bairdi*), and Pacific halibut (*Hippoglossus stenolepis*) (Mondragon and others, 2007a,b). Seafloor substrates and, therefore, potential benthic habitats were mapped at depths ranging from just below the surface to greater than 400 m in the deepest fjord basins. The substrate was characterized by using a combination of high-resolution multibeam bathymetry and backscatter imagery, numerous groundtruthing sources, and knowledge of the local fjord environment.

The multibeam data used in this study were collected aboard the National Oceanic and Atmospheric Administration (NOAA) ship, *Fairweather,* during NOAA National Ocean Service (NOS) hydrographic surveys H12140, H12141, and H12142. Additional groundtruthing was conducted using camera sled and ROV (remotely operated underwater vehicle) aboard the R/V *Steller,* cruise S-T3-10-GB, in September, 2010. Groundtruth transects were selected based on visual inspection of the NOS bathymetric and backscatter intensity data. These observations are supplemented with preexisting bottom-grab and sediment-core descriptions, available in the Index to Marine and Lacustrine Geological Samples database, maintained by the National Geophysical Data Center (NGDC; last accessed in 2012).

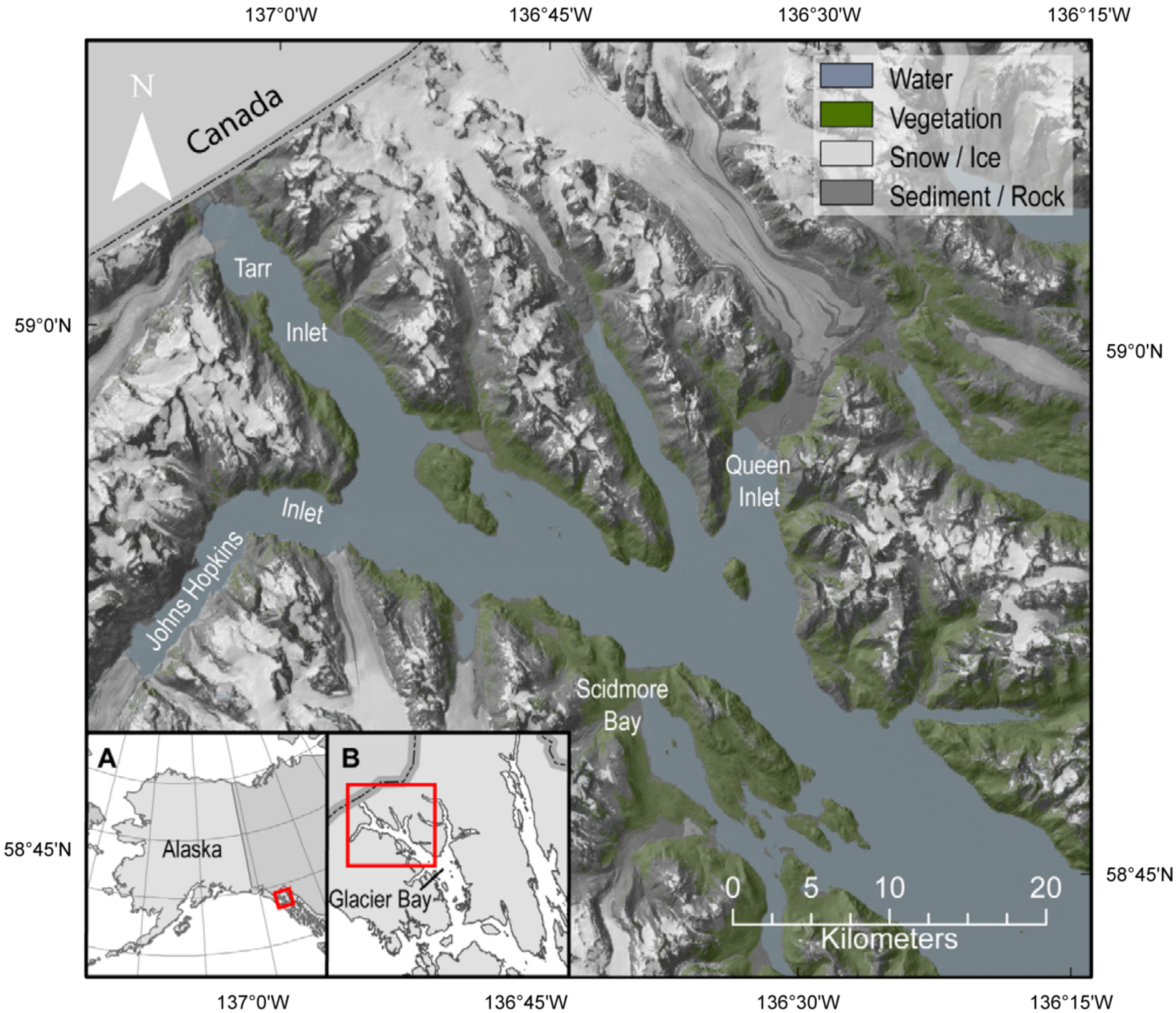

Figure 1. Location maps for the West Arm relative to (*A*) Alaska and (*B*) Glacier Bay.

The multibeam bathymetric and acoustic backscatter data were compiled with additional information in an ESRI (2005) Geographic Information System database to create several map products. NOAA and NatureServe Coastal and Marine Ecological Classification Standard (CMECS; Madden and others, 2008) was used to classify seafloor substrate, potential benthic habitats, water column properties, and seafloor geomorphology (Madden and others, 2009). An additional map of modern sediment flux measurements using quantitative differential bathymetry is also presented. These maps serve as baselines for further research and have implications for park management.

Setting

Glacier Bay National Park & Preserve is located in southeastern Alaska (fig. 1). It is a fjord system that bifurcates into two main northern tributaries: the West Arm and Muir Inlet, also known as the East Arm. This study focuses on the West Arm, a 58-km-long system of fjords, including Tarr, Johns Hopkins, Queen, Reid, and Tidal Inlets, which have recently undergone well-documented rapid deglaciation (Powell, 1984; Hall and others, 1995). The West Arm is a highly dynamic estuarine environment owing to its recent deglaciation, high sedimentation rates, and vigorous tidal currents—forces that affect seafloor stability and constantly shape benthic environments. This diverse settings is also host to productive food webs; recreational, commercial, and subsistence fisheries; large populations of marine mammals and seabirds; and vessel-based tourism (Piatt and Gende, 2007).

Geology

Glacier Bay is surrounded by three large mountain ranges—the Chilkat Range to the east, the Takhinsha Mountains in the north, and the Fairweather Range to the west—that separate the fjord system from the Gulf of Alaska. The park is set in a tectonically active area with several nearby active fault systems including the Chilkat-Chatham Strait Fault to the east, the Queen Charlotte-Fairweather Fault to the west, and the Border Ranges Fault that runs through parts of the West Arm (Powell, 1984). Upper Glacier Bay is undergoing glacial isostatic uplift at a rate of 25 mm/yr due to post-Little Ice Age ice loss (Larson and others, 2004). The regional bedrock geology is complex, with a range of rock types and origins, including metasedimentary rocks intruded by younger granitic plutons. Geological units exposed at the surface surrounding the West Arm are predominately Tertiary and Cretaceous granite; granodiorite and diorite; Cretaceous, Silurian, Devonian, and Permian metasedimentary rocks; and Quaternary sediment (Powell, 1984).

Temperate Glacimarine Environment

The cool to temperate maritime climate of southeast Alaska and very high, tectonically active mountain ranges permit widespread glaciation at a relatively low latitude (Wilson and Overland, 1987). Abundant precipitation in the form of snow in the surrounding mountain ranges feeds many valley glaciers that flow into Glacier Bay that are among the largest and most active in southeast Alaska. The glaciers of this region are temperate and characterized by seasonally abundant meltwater that carries high sediment loads to produce large depositional landforms (for example, Goldwait, 1974; Powell, 1991; Hunter, 1994). Significant research has focused on the rich glacimarine sedimentary record within Glacier Bay, yielding insight into complex glacimarine processes (for example, Powell, 1991; Hunter and others, 1996; Cowan and others, 1999) and the history and processes of deglaciation (Seramur and others, 1997).

Glacial sediment fluxes from the temperate glaciers in southeast Alaska are among the highest recorded worldwide (Powell and Molnia, 1989; Hallet and others, 1996; Elverhøi and others, 1998). Extreme rates of sediment accumulation, in some instances in excess of 80 m/yr, have been documented near glacial termini in the region (Powell, 1991; Hunter and others, 1996; Cai and others, 1997; Seramur and others, 1997) and decrease very rapidly with distance from the terminus (for example, Syvitski, 1989). A proper understanding of these rates is important because of their potential paleoclimatic significance (Cowan and Powell, 2007) and their affect on glacier stability (Powell, 1991) and also because such high clastic sedimentation may be a major physical control on the diversity and spatial distribution of fjord biota (for example, Carney and others, 1999; Wlodarska-Kowalczuk and Pearson, 2004).

The post-Little Ice Age deglaciation in the region has occurred at some of the highest rates documented worldwide. Nearly 100 km of glacier retreat during the past two centuries has left behind a network of canals, moraines, outwash complexes, and large volumes of glacimarine sediment. Prior to 1860, the glaciers of the West Arm and Muir Inlet formed a confluent tidewater glacier complex near Tlingit Point. From 1860 to 1892, the ice front receded rapidly by at least 1.8 km/yr, dividing into two distinct fronts near the junction of Tarr and Johns Hopkins Inlets sometime between 1879 and 1892 (Cai, 1994). By the late 1920s, the ice fronts terminated roughly 2 km upfjord from their modern positions. The retreat of Johns Hopkins Glacier ended by about 1926. In Tarr Inlet, the retreat of Grand Pacific Glacier continued until the early 1940s. Since that time, the termini of the West Arm glaciers have been advancing or quasi-stable (Hall and others, 1995; Powell, 1984; Powell, 1991), fluctuating asynchronously, apparently controlled by autogenic factors such as glacier dynamics and channel geometry rather than climate (Powell, 1984, 1991).

Oceanography

The oceanographic setting of Glacier Bay is also complex, owing to the concurrence of bathymetric variability, tidal currents, and strong seasonal stratification resulting from high rates of glacial ablation, snow melt, and precipitation (Hooge and Hooge, 2002; Etherington and others, 2007a). The morphology of the West Arm is characteristic of a glacial fjord and includes a shallow sill topped with a glacial morainal bank complex at its mouth (Seramur and others, 1997), steeply sloping walls up to 77°, and multiple deep basins separated by transverse sills and morainal banks.

Areas of shallow bathymetry influence tidal current velocity and vertical mixing (Etherington and others, 2007a). In contrast, deep basins are highly stratified in the pelagic environment and have minimal benthic currents. Average root mean square (RMS) current speeds (derived from an advanced circulation, or ADCIRC, tidal circulation model) for the main stem of the West Arm are small, ranging from 0.001 to 0.043 m/s. However, peak instantaneous velocities are approximately 50 to 100 percent higher than RMS velocity values, particularly over areas of shallow bathymetry (Etherington and others, 2007a; Hill, 2007). Model results demonstrate the large tidal range within Glacier Bay, with values averaging 3.86 m at the lowest portions of the Bay, increasing with distance up the arms of the Bay, and reaching an average of 4.59 m at the head of the inlets (Hill, 2007; Etherington and others, 2007a). The highest tides in the Bay are found in Adams Inlet (Hill, 2007). Glacier Bay exhibits mixed tides, with two high and two low tides per day and with successive high and low tides of varied amplitude (Etherington and others, 2007a).

Freshwater input at the head of the fjord is a dominant driver of water-column stratification (Etherington and others, 2007a). Spatial and seasonal variability are greatest for salinity and stratification and are directly associated with freshwater flux (Etherington and others, 2007a; Hill and others, 2009). This flux peaks between June and October at about 1,000 m^3/s for the entire Glacier Bay watershed (Hill and others, 2009). The summer discharge peak coincides with peak stratification, peak water temperature, minimum surface salinity, and generally higher chlorophyll *a* concentrations (Etherington and others, 2007a). Likewise, peak glacimarine sediment flux also occurs during the summer months due to enhanced subglacial stream discharge (Cowan and Powell, 1990).

Freshwater flux from glacial ablation is both important to local fjord conditions (Etherington and others, 2007a; Hill and others, 2009) and globally, because the glaciers of southeast Alaska account for 15 percent of present-day eustatic sea level rise (Meier and others, 2007). The thinning of southeast Alaskan glaciers contributed 0.04±0.01 mm/yr to global sea-level rise in the latter part of the 20th century (Larson and others, 2007). More recently, mass loss from these glaciers was found to contribute 0.23±0.01 mm/yr to global sea-level rise for the period April 2003 through March 2007 (Luthcke and others, 2008).

Previous Habitat Mapping in Glacier Bay

Several benthic habitat mapping initiatives have been completed in Glacier Bay proper. In 2001, the U.S. Geological Survey (USGS) collected multibeam bathymetry for this area (Carlson and others, 2002). In 2004, ground-truth-data were collected to supervise an effort to correlate seafloor geology and biology. This work included seafloor video observations and sediment sampling and resulted in a characterization of seafloor morphology, substrate, and habitat distribution following the Greene and others (1999) classification scheme (Harney and others, 2007).

Subsequent research based on these data includes a geological to biological association analysis by Etherington and others (2007b). This work used detrended correspondence analysis, a multivariate statistical technique, to examine relations between habitat types and taxa distribution. Etherington and others (2007b) found substrate type and current exposure to be the dominant control on species distributions in Glacier Bay. Three benthic habitats were identified: (1) shallow-water, high-current sand and cobble habitat associated with urchin, horse mussel, and scallop; (2) deep-water mud habitat associated with gastropod, algae, flatfish, Tanner crab, shrimp, sea pen, and other crustaceans; and (3) moderate-depth cobble and mud habitat associated with sea star, rockfish, sculpin, anemone, sea cucumber, worm, pollock/cod, basket star, and other fish (Etherington and others, 2007b).

The pilot study for the project, undertaken by Trusel and others (2010), mapped seafloor geology in Muir Inlet, relating factors such as water depth, glacial proximity, and seafloor morphology with the spatial and temporal distribution of benthic habitats.

Coastal and Marine Ecological Classification Standard

The Coastal and Marine Ecological Classification Standard (CMECS), developed by NOAA and NatureServe, was proposed as a national standard for classification of coastal and marine resources, adhering to the Federal Geographic Data Committee (FGDC) in 2008. CMECS encompasses five individual components to cover all aspects of the marine environment: surficial geology, water column, geoform, sub-benthic, and biotic cover. Results presented here focus on the surficial geology component and the geoform component but also include preliminary application of the water column component and adhere to the guidelines of CMECS Version III (August 2009 draft version, Madden and others, 2009). The surficial geology component (SFG), the primary component, is a hierarchical scale-based system that describes geomorphological, physico-chemical, and biological compositions of the coastal and marine substrates (Madden and others, 2009). The water column component (WCC) describes the structure, processes, and biology of the water column. The geoform component (GFC) describes the coastal seafloor geomorphology at different scales (Madden and others, 2009).

Data Sources

Multibeam Sonar

Benthic habitat and seafloor substrate mapping for the West Arm were conducted using multibeam sonar data collected onboard the NOAA ship, *Fairweather,* during NOAA NOS hydrographic surveys H12140, H12141, and H12142 in late September through early November 2010. The *Fairweather* employed A Reson 7111 multibeam for the purpose of high-resolution bathymetric surveying. Data were processed using CARIS HIPS & SIPS v 7.0, Service Pack 1, Hotfix 5, cleaned for errant points, referenced to mean lower low water (MLLW) by correcting for tide, and finally transformed into depth versus absolute position. MLLW was locally determined by tide stations installed at Composite Island and Tarr Inlet. The operating National Water Level Observation Network (NWLON) primary tide station at Elfin Cove, AK (945–2634), served as control for datum determination (NOAA 2009a,b,c). For a more detailed discussion of data processing/acquisition and quality control procedures, refer to the descriptive reports that accompany each survey or NOAA ship, *Fairweather,* 2009 Data Acquisition and Processing Report (DAPR). Bathymetry and backscatter data were gridded using 16-m horizontal grid resolutions. About 381 km^2 or 93 percent of the West Arm is covered by bathymetric data, extending from just below sea level to over 400 m depth in the lower West Arm fjord basin and from Tlingit Point to the heads of Tarr and Johns Hopkins Inlets.

Groundtruthing Information

Groundtruthing operations were conducted aboard the R/V *Steller* in late August and early June of 2010. USGS seafloor observations, collected via towed video sled, provided the primary ground-truth source for this study (see cruise report at *http://walrus.wr.usgs.gov/infobank/s/st310gb/html/s-t3-10-gb.meta*). Transects were selected to ground truth across the full spectrum of depth, slope, and rugosity observed in the multibeam bathymetry. Selection was oriented toward resolving both common and unique features of the seafloor and examining regions of transition between different substrate types. Video observations were subsequently used to construct maps of substrate type and habitat distribution.

The video sled was equipped with forward- and downward- facing video cameras, lights, an altimeter, and a pressure (depth) sensor. Two down-pointing lasers, spaced 20 cm apart, provided scale in the seafloor imagery. The sled was towed behind the surface vessel at speeds of 0.5–1.5 kn, generally operating at an altitude between 1 and 2 m above the seafloor. Video footage was recorded to digital mini-DV tape, which was continuously imprinted with altitude, pitch, roll, water depth, ship latitude and longitude, ship speed, ship heading, and Greenwich Mean Time (GMT). Ship position was determined by differential geographic positioning system (dGPS). All instrument data were multipexed through a sub-sea housing and transmitted by the 12-conductor cable to a topside console.

Real-time seafloor observations were recorded using an X-keys programmable keypad at 1-minute intervals during each transect following the methodology of Anderson and others (2008). Time (GMT), ship position, and other ship data were automatically recorded each time an observation event was entered. Positional data in the observation file were later corrected to true sled position, determined using a Linkquest Tracklink 1500, which provided sled position relative to the ship-board dGPS. Observations at each point included primary and secondary substrate type (for example, mud/mud, boulder/cobble), substrate complexity (rugosity), seafloor slope, benthic biomass, the presence of benthic organisms and demersal fish, and small-scale sea-floor features (for example, tracks and burrows).

In areas of complex bathymetry and substrate, the limited maneuverability granted by the tow sled was often insufficient for reliable and continuous data collection. Such transects were completed using a Benthos Stingray ROV. Due to the limited range imposed by the 400 umbilical, the ROV occupied an auxiliary role during groundtruthing investigations. The buoyancy provided by the Stingray platform was inadequate for the equipment of the Tracklink positioning transducer. As a result, ROV observations are given with ship position only. Because the ROV was tethered to a clump weight lowered beneath the ship, true ROV position is constrained to within ~100 m of the ship's position.

In addition to the seafloor video transects, 127 bottom-grab samples (available in the NGDC's Index to Marine & Lacustrine Geological Samples—*http://www.ngdc.noaa.gov/mgg/curator/*), seismic-reflection profiles (Cowan and others, 1994; Cai, 1994), and Landsat imagery also aided in the interpretation of the multibeam data. In particular, an understanding of modern processes active in the glacimarine environment was fundamental to our interpretations, especially in areas of poor coverage.

Methodology

Surficial Geology Component

The classification of seafloor habitats was performed using a supervised manual classification of seafloor substrate based on knowledge from groundtruthing sources (fig. 2): two derivative bathymetric properties (seafloor rugosity, fig. 3) and slope (fig. 4). Multibeam backscatter supplemented the primary data sets in locations where surficial geology was ambiguous. However, due to the low quality of the backscatter in the West Arm, we were unable to replicate the approach employed in Muir Inlet, where backscatter intensity was used to infer substrate distribution (see Trusel and others, 2010). Instead, our approach relies heavily on groundtruthed data collected during this study and previous NOS cruises.

Seafloor rugosity (fig. 3) was calculated using IVS 3-D Fledermaus. Rugosity is a dimensionless measure of seafloor roughness or its actual surface area divided by its planar area. Therefore, a completely flat surface has a rugosity of exactly 1. In general, a higher rugosity is characteristic of rough substrates such as rocky areas. Likewise, lower rugosity is characteristic of flat, less complex, soft-bottom substrates. The second derivative bathymetric measurement is seafloor slope (fig. 4). Because of sediment instability on steep slopes, areas with very high slope are often consolidated glacial material or bedrock, whereas low sloping areas are the loci of soft-sediment deposition and redeposition from slope failures and sediment gravity flows from fjord walls.

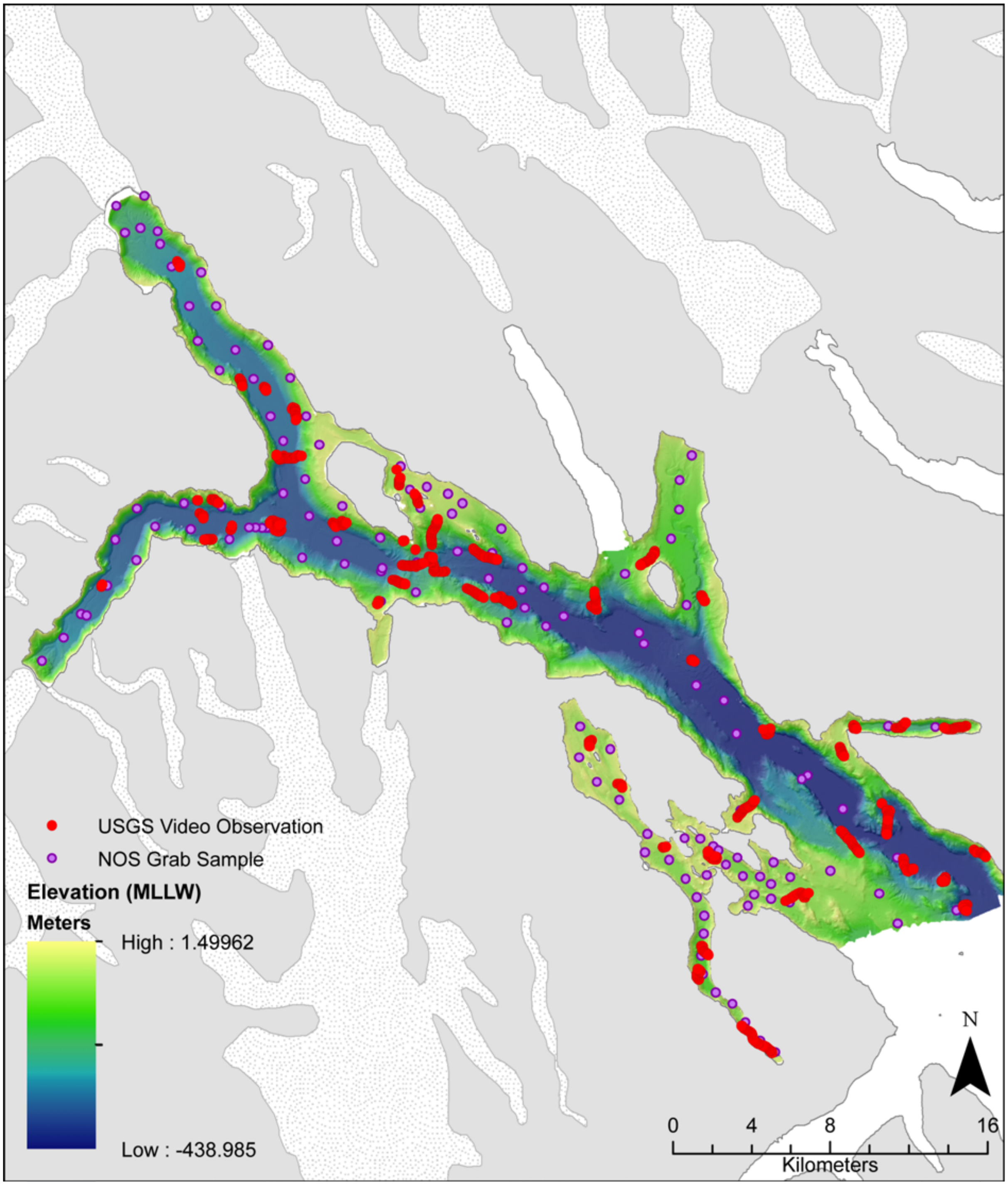

Figure 2. Map of USGS Video Observations and NOS Grab Samples.

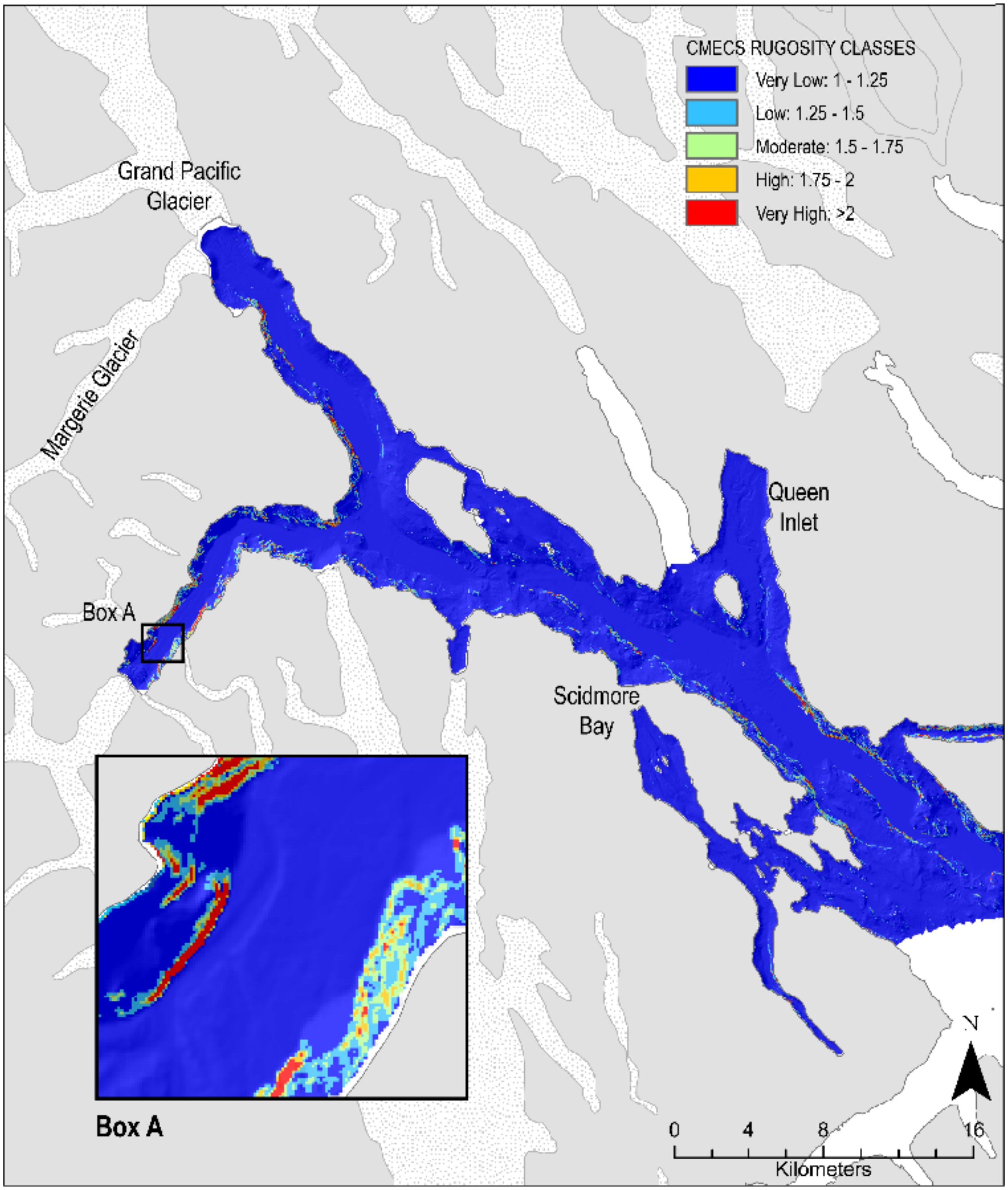

Figure 3. Map of CMECS rugosity classes for the West Arm.

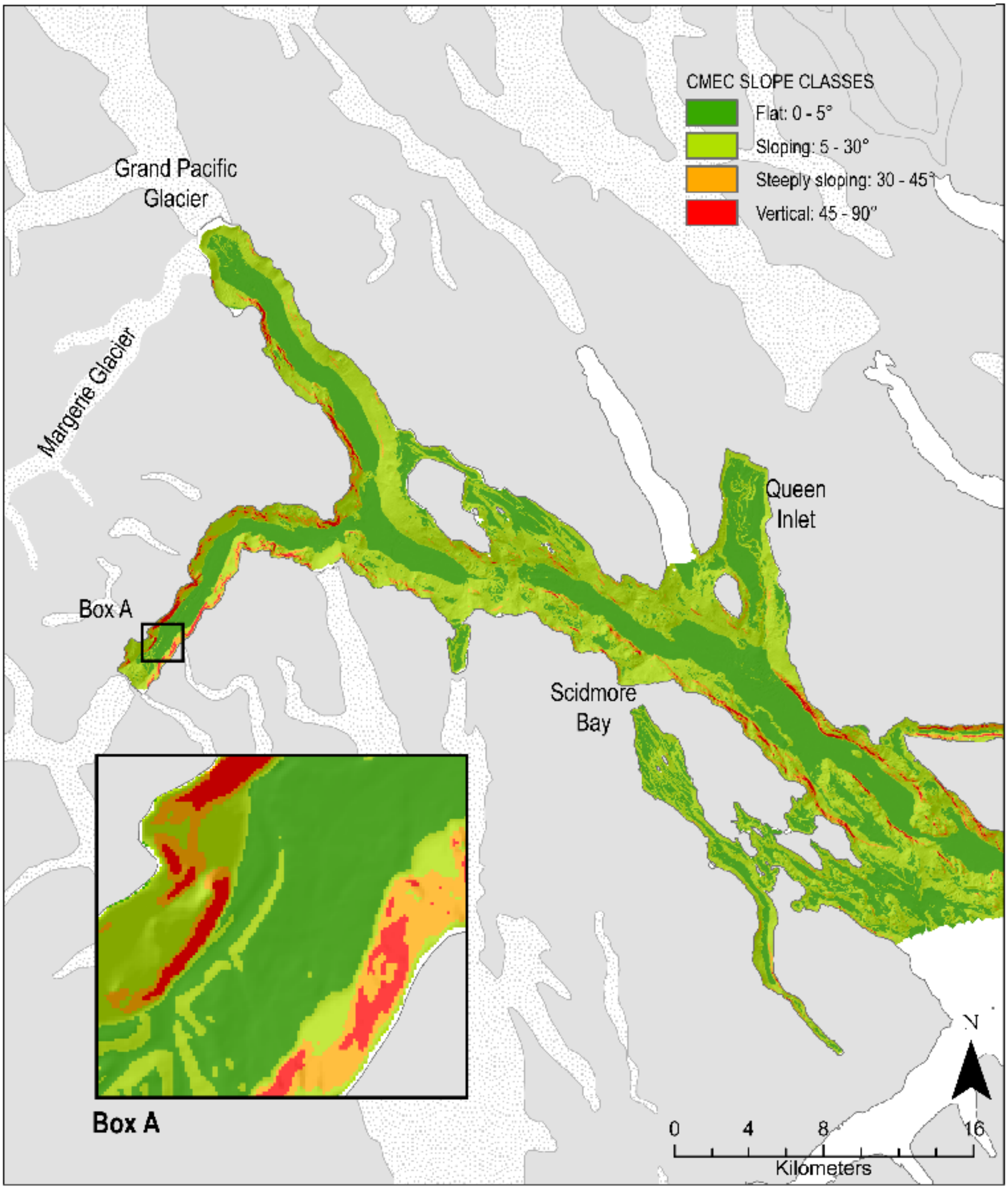

Figure 4. Map of CMECS slope classes for the West Arm.

Rugosity and slope rasters were both reclassified into groups according to CMECS such that areas with similar rugosity or slope are combined into classes (figs. 3, 4). Rugosity is a somewhat qualitative measurement that is biased based on the resolution of the bathymetry, that is, a rugosity value obtained with 16-m^2 resolution will be different for the same area using 5-m^2 bathymetry data. Therefore, rugosity classes may be altered in specific applications to better represent the data (for example, Greene and others, 2007). We chose to modify the CMECS classes to better represent variability within our rugosity measurements (tables 1–3).

Historical Bathymetric Data

Two historical bathymetric datasets were used to measure recent sediment accumulation within the West Arm. NOAA NOS hydrographic surveys H09315 and H09316, collected in August 1972 aboard the NOAA ship, *MacArthur*, cover Johns Hopkins and Tarr Inlet respectively (NOAA 1972a,b).

Table 1. CMECS slope classes.

Slope	Vertical angle[1]	Percentage of total area	Area (km^2)
Flat	0–5°	41.4	159.2
Sloping	5–30°	51.5	197.9
Steeply sloping	30–45°	5.4	20.8
Vertical	45–90°	1.7	6.4
Overhang[1]	>90°	0	0

[1] The greatest slope measured in the West Arm was 72.8°.

Table 2. CMECS rugosity classes surveyed within the West Arm.

Rugosity types	Values[1]	Percentage of total area	Area (km^2)
Very Low	1–1.25	94.4	356
Low	1.25–1.5	3.4	12.8
Moderate	1.5–1.75	1.1	4.3
High	1.75–2	1.9	1.9
Very high	>2	2.2	2.2

[1]Modified rugosity values based on Madden and others (2008) and Greene and others (2007).

Table 3. CMECS benthic depth zones surveyed within the West Arm.

Benthic depth zone	Water depth range (m below sea level)	Percentage of total area	Area (km^2)
Shallow infralittoral	0–5	0.1	2.3
Deep infralittoral	5–30	7.7	29.6
Circalittoral	30–80	16.2	62
Circalittoral (offshore)	80–200	25.4	97.4
Mesobenthic	200–1,000	50.2	192.5

Historical bathymetric data from the lower West Arm and its tributaries were obtained from NOS hygrographic surveys H09138, H09139, H09141, H09142, H09143, collected in June through August of 1970 aboard the NOAA ship, *Fairweather* (NOAA 1970a,b,c,d,e). Both datasets were collected using Raytheon DE-723 fathometers for depth measurements. Sounding velocity corrections were determined using serial temperature and salinity. In Johns Hopkins and Tarr Inlets, velocity corrections were less than 0.5 percent of the sounding depth for the entire survey area and, therefore, velocity corrections were not applied to surveys H09315 and H09316 (NOAA 1972a,b). Depth measurements were corrected for tidal state and referenced to MLLW. Locations were determined using visual three-point sextant fix methods. Hydrographic signal positions were established using a WANG Model 700 Calculator in conjunction with the WANG Geodetic Program Library (NOAA 1972a,b).

A preliminary surficial geologic map was constructed using a maximum likelihood classification (MLC) based on slope, geoform, and groundtruthing observations. Our approach relies on the assumption that geoform and slope (angle of repose) are often indicative of substrate; the primary caveat is that a feature may be draped in one sediment type, while the morphology is inherited from the underlying material (for example, mud draping a steep bedrock outcrop). To reduce misclassification by the MLC, the possible substrate types were initially limited to two general induration classes: rock bottom and unconsolidated bottom. The resulting map provided the template for subsequent manual classification. Flat to sloping areas classified as rock bottom were investigated and changed to unconsolidated bottom when supported by ancillary data or geological reasoning. Similarly, steeply sloping and vertical areas classified as unconsolidated bottom were reclassified to rock bottom if reasonable.

Further classification was completed in the surficial geology component down to the subclass level, where unconsolidated bottom was divided into mud, sand, mixed sediments, and cobble/gravel. Rock bottom was further divided into bedrock and boulder/rubble. Considering the extreme predominance of glacimarine sedimentation in the West Arm and groundtruthing that confirmed substrates dominated by mud (silt and clay) for all basin floor areas, the unconsolidated bottom class was first characterized as entirely mud. We assume most areas in the West Arm are veiled in mud, an inference supported by groundtruthing data. Lacking abundant physical samples or imagery of any soft bottom material other than mud, geological reasoning was used to classify other unconsolidated bottom subclasses. Numerous side-input fluvial sources enter the West Arm and often manifest in fjord-edge deltas. Transport channels on the delta slopes are evident in the backscatter as having a higher intensity relative to the surrounding cover. We assume most of these deltaic sources transport sand-sized particles into the fjord although samples are lacking for many locations, and thus these areas were typically classified using the CMECS sand subclass. Notable exceptions to this rule of thumb include Johns Hopkins and Tidal Inlets, where the steep topography introduces larger clasts into the deltaic environment. Such areas were classified as either cobble/gravel or unclassified soft bottom depending on the availability of groundtruthed observations. The sand subclass was also applied to active morainal banks. In this environment, the turbidity of the water column limited the effectiveness of video observation. While processes such as dumping and gravity flows contribute coarser sediments near the terminus, studies of temperate glacimarine environments (Cai, 1994; Hunter, 1994) suggest that the morainal core still falls within the CMECS definition of the sand subclass. In subclassifying the rock bottom class, all areas were initially assumed to be bedrock. Bedrock areas were groundtruthed using seafloor observations (this study), seismic reflection data (Cai, 1994), or observation of transitions of subaerially exposed steep bedrock cliffs into the submarine environment. Areas of apparent submarine talus were identified through fine scale investigation and classified as boulder/rubble (fig. 5). Most commonly, boulder/rubble exists at the base of submarine bedrock cliffs and is characterized by a lower slope than the bedrock and a lobate, splay geometry. These are inferred to form from rock falls and slides that originate both above and below water.

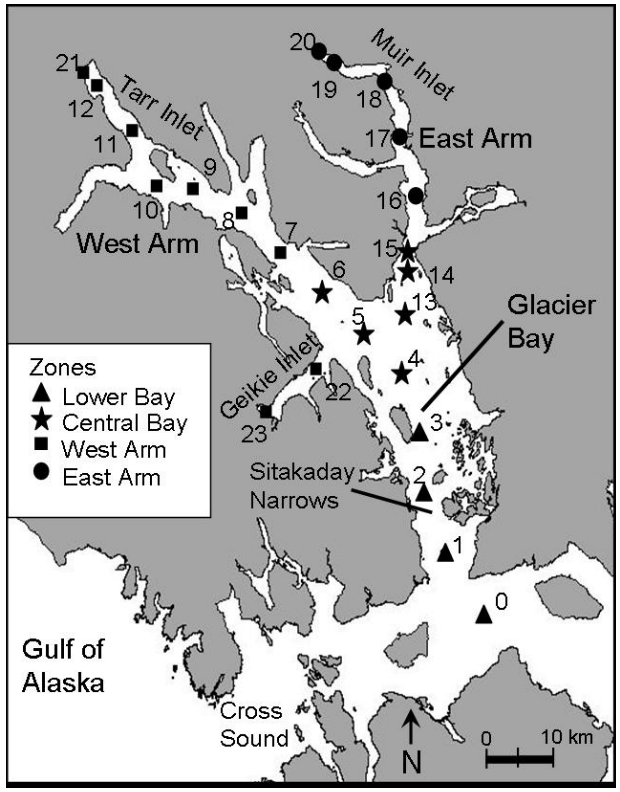

Figure 5. Glacier Bay oceanographic stations (Trusel and others, 2010, adapted from Etherington and others, 2007a).

Geoform Component

Geoforms in the West Arm were manually selected from the multibeam bathymetry data with the aid of video observations, knowledge of glacimarine processes, well-documented glacial history in the West Arm, and interpretations from other studies (for example, Cai, 1994). Spatial scales defined within the CMECS framework were used to define linear scales using the largest measurable axis. Geoforms were only characterized down to the mesogeoform level (tens of meters to kilometers in size) because of the limited resolution of our bathymetric data. Many areas in the West Arm fit into more than one megageoform and mesogeoform class. For example, the West Arm lies within the continental margin megageoform, but it is also a fjord megageoform. At the mesogeoform level, a fjord wall is a mesogeoform, but the wall also has multiple mesogeoform-scale bedrock outcrops and other features. Therefore, when delineating polygons, it was necessary to have multiple megageoform and mesogeoform categories. These are listed in the GIS table as “MEGA_GF”, “MEGA_GF_2”, and so forth. While multiple geoforms were selected for each spatial scale, a primary and most informative geoform was chosen for display at each scale; these are listed in the GIS table as “DISPMEGAGF” and “DISPMESOGF”. Because all smaller geoforms lie within the fjord megageoform, the primary mesogeoform is shown in sheets 3 and 4. The CMECS benthic depth zones divide many of these mesogeoforms. To aid in visualization, the color shade of each geoform type gets darker as depth zone increases.

Water Column Component

Following the CMECS system, water-column classes and attributes were assigned to locations of established oceanographic stations within Glacier Bay (Etherington and others, 2007a). Two main data sets were used to define classes and attributes: (1) conductivity temperature depth (CTD) data (Etherington and others, 2007a) and (2) results from a tidal circulation model (Hill and others, 2009; Hill, 2007). Results of the tidal circulation model were used to classify the CMECS attributes of tidal range and energy intensity, whereas the CTD data were used for all other water-column attributes. Model predictions of water elevation have been validated against several NOAA stations within Glacier Bay and resulted in strong agreement between predicted and measured values. Model predictions of tidal velocity have been compared with minimum and maximum values of velocity at several NOAA stations within Glacier Bay, and the model showed general agreement.

CTD data were collected at 22 stations spanning the axes of Glacier Bay from 1993 to 2002 and covering all seasons (fig. 6). Parameters include salinity, temperature, density/stratification, turbidity, photosynthetically available radiation, and chlorophyll *a*. This set of eight stations (6–12 and 21) spans the length of the West Arm's mainstem through Tarr Inlet. Detailed computational tidal simulations of Glacier Bay were conducted using an ADCIRC tidal circulation model (Hill, 2007; Hill and others, 2009). ADCIRC output includes time series and global output of water-surface elevation and depth-integrated velocity. To determine a single representative value of tidal-current speed and tidal range at each oceanographic station, the RMS values of speed and tidal elevation were calculated from the results of a harmonic analysis of the model domain (Hill, 2007).

The framework for the CMECS water column component is in draft form and additional work is needed to refine it and develop the rules for combining classifiers to identify and describe the water column units (Madden and others, 2008). As a result, this study will employ the approach developed for habitat mapping in neighboring Muir Inlet (Trusel and others, 2010). The structure of the water column was used to define two vertical strata—upper water layer and bottom water layer—which are defined by those strata above and below the pycnocline, respectively. The pycnocline within Glacier Bay varies both spatially and temporally but generally exists at 15 m depth or shallower. Because temporal averages were used to define the water-column properties and to simplify the classification of water layers, the upper water layer was defined as 0–15 m below the surface while the bottom water layer was the remaining water column below this stratum. This standard definition was used for all oceanographic stations of Glacier Bay, and average oceanographic parameter values from 0 to 15 m were used to classify the upper water layer.

CMECS water-column classes and general attributes were applied to the upper water column and bottom water column separately for each of the oceanographic stations. All attributes that contained data

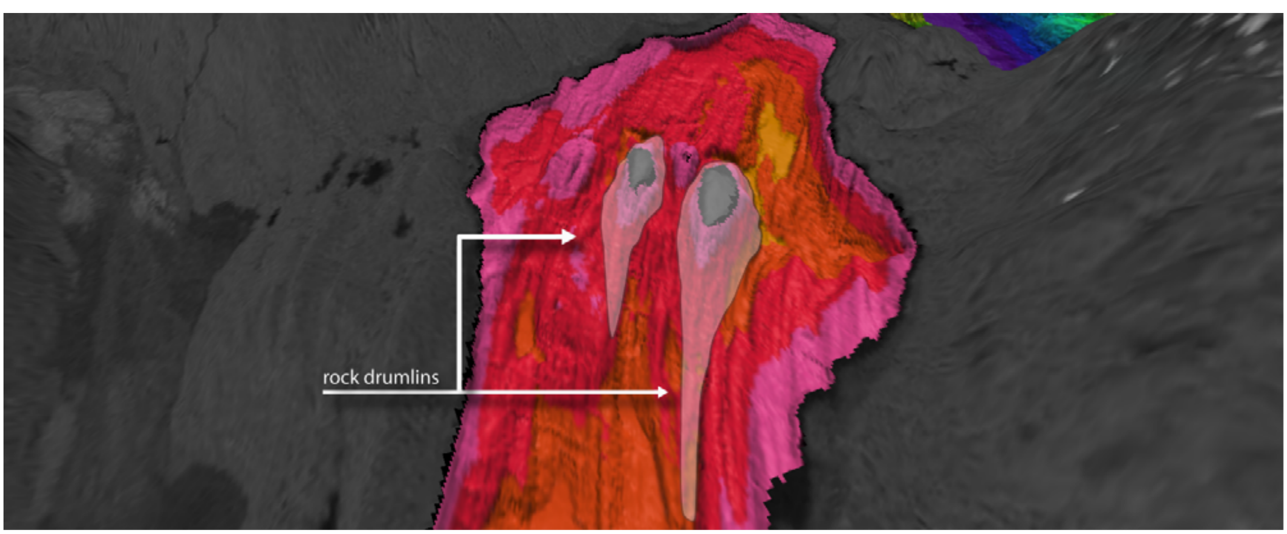

Figure 6. Rock drumlins and other streamlined features in Scidmore Inlet.

were assessed and classified. Averages of parameters over tidal conditions (for example, ebb/flood, spring/neap) and various time scales (months, years) were used to classify each oceanographic station. The output of tidal velocity from the tidal circulation model is used to classify energy intensity in the upper water column. In shallower areas where vertical mixing is apparent and tidal energy is higher (Etherington and others, 2007a; Hill and others, 2009), bottom energy intensity is assumed to mirror surface energy intensity, and depth-integrated velocity values are used to also classify energy intensity in the bottom water-column stratum. In deeper areas where stratification is higher and tidal energy is lower (Etherington and others, 2007a; Hill and others, 2009), energy intensity within the bottom water column-stratum is classified as no energy. Visual observations of virtually no current motion and accumulation of fine sediments in these deeper areas support this assumption (Etherington and others, 2007b; Harney and others, 2007). Values were only assigned to a point location and were not extrapolated beyond the oceanographic station; thus, only the central regions of the inlets of Glacier Bay were classified. Therefore, the water-column classification differs from the geoform and benthic cover classifications, which were based on a comprehensive continuous data set covering almost the entirety of the West Arm.

Sediment Accumulation

Sediment accumulation rates for most of the West Arm were calculated using quantitative differential bathymetry. Three bathymetric datasets were used: the 2009 multibeam bathymetry used in this study for seafloor characterization and the 1970 and 1972 singlebeam bathymetry from NOAA NOS hydrographic surveys. Average sediment accumulation rates were calculated by subtracting the depths from 2009 from those measured in 1970/72 and then dividing by the time period. For this study we are interested in modern sedimentation rates because of their potential as a limiting factor in the distribution and diversity of benthic biota (for example, Carney and others, 1999; Wlodarska-Kowalczuk and Pearson, 2004).

Because poor between-track spatial resolution is often associated with the singlebeam collection methods in the NOS data, the historical bathymetric data points were manually modified to artificially increase fjord basin-edge resolution. While geographic locations of the historical soundings are potentially highly accurate (see Umbach, 1976), even minor errors in horizontal location over variable-relief bathymetry can lead to large errors in depth measurement. This potentially problematic scenario is avoided by making measurements only over the very low relief and slope basin floor areas, where poor between-track data coverage is not critical.

The 1970 and 1972 bathymetric grids were differenced with the 2009 multibeam bathymetry using ArcGIS over the low relief and low rugosity fjord-floor areas. In general, basin floor areas were delineated as having a slope of less than 5°. The resulting sediment-thickness grid was divided by 39 and 37 years (1970 to 2009 and 1972 to 2009, respectively) to calculate an average annual sediment accumulation rate between elapsed surveys.

We assume that the flat fjord floor character has remained relatively constant and that the primary temporal change has been basin-floor aggradation. This assumption is supported by seismic profiles showing thick and continuously well-stratified glacimarine sediment horizons in the deep basins of the West Arm that onlap adjacent walls and bathymetric highs (for example, Cai, 1994; Cowan and others, 1999). We also assume that the bulk of sediment accumulation occurs in the fjord-floor basins, either through direct deposition from glacimarine suspension settling or through redepositional events from slope failures, sediment gravity flows, and other mass movements, processes common to fjords (for example, Powell and Molnia, 1989; Syvitski, 1989). Using these two assumptions, we have modified the results of the differential bathymetry analysis by extrapolating the resulting sedimentation rates to the edges of the fjord-floor basins as defined in the 2009 multibeam data. These modified data were interpolated and gridded using the natural neighbor interpolation function within ArcGIS. In effect, this method simply extrapolates from the relatively accurate data in each basin, reducing the affect of erroneous soundings. The result is a relatively planar surface that mirrors the basin floor morphology.

Results and Discussion

Surficial Geology Component

Results of the subclass level SGC mapping for the West Arm are shown in sheets 1 and 2. Coverage for the SGC substrate classification is summarized for the entire fjord (table 4). As expected, unconsolidated bottom types dominate the West Arm, owing to the large glacimarine sediment flux from Tarr and Johns Hopkins Inlets. Seventy-two percent of the West Arm is covered by mud, far more than any other bottom type. The second most abundant substrate in the West Arm is unclassified unconsolidated bottom, which composes about 14 percent of mapped substrate. The more general unconsolidated bottom class was typically applied where groundtruthing coverage was poor but higher energy processes, such as tidal winnowing, are suspected to disrupt hemipelagic sedimentation. Prominent examples include the shallows of Hugh Miller Inlet and along many of the steep fjord walls. The latter environment falls under the influence of gravity flows and rock falls rather than tidal winnowing. The sand subclass covers 3.0 percent and typifies the foresets of side-wall and fjord-head deltas and active morainal banks. The latter environment likely includes a large component of other size fractions that reflect processes, including dumping and gravity flows (Hunter, 1994), yet still conforms to the CMECS definition of the sand subclass. Areas where no single size fraction constituted the majority of the substrate fall under the mixed sediments subclass. Mixed sediments, composing 1.6 percent of the West Arm, are primarily found in the shallows of Hugh Miller Inlet and at the mouth of Tidal Inlet, where winnowing has exposed ice-contact sediments deposited during the post-Little Ice Age retreat of the Russell System. Of the two rock bottom subclasses, bedrock is the most abundant, constituting 7 percent of the West Arm and 98 percent of the rock bottom class. Boulder/rubble could be confidently mapped in only 0.2 percent of the study area. This disparity may be partially attributable to the distribution of observation points, as steep fjord walls posed a significant hazard to groundtruthing operations in shallow water. Such environments are suspected of having a significant boulder/rubble component owing to the combination of rock falls and current winnowing. The true abundance of the boulder/rubble substrate likely falls within one order of magnitude of the value presented in table 4, which constitute <2 percent of the West Arm.

The summary of substrates for each CMECS depth zone illustrates the types of benthic habitats available at different depths within the West Arm (table 5). The majority of rock bottom substrates are located in the circalittoral (offshore) and mesobenthic depth zones. This is expected, because the fjord walls are predominantly located within these depth zones (table 5). Likewise, the vast majority of mud falls within the mesobenthic depth zone, which is dominated by fjord basin floors. Despite the inherent relation between mud and the fjord floor class, a large discrepancy exists between their abundances, roughly 72 percent and 34 percent, respectively, attributed to the fact that hemipelagic sediment tends to drape low energy environments, regardless of the underlying geoform. Shallower, higher energy environments, where the finer hemipelagic component is winnowed out, are more typically associated with the mixed sediments and unclassified unconsolidated bottom classes. The relative distribution of these substrates reflects this, exhibiting the greatest abundances in the depth zones above 200 m. The 26.8 km^2 of mixed and unclassified sediments found within the circalittoral (offshore) and mesobenthic zones (80–1,000 m) are suspect and may, in fact, be dominated by mud. In general, the application of these classes within the deeper depth zones was reserved for sites where the substrate is suspected of varying temporally, such as at lower delta forsets and proximal to steep bedrock cliffs. In the former

Table 4. Substrate distribution for the West Arm.

CMECS class	CMECS subclass	Percentage of total area	Area (km^2)
Unconsolidated Bottom	Unclassified	14.4	55.4
	Mud	72.0	276.6
	Sand	3.0	11.8
	Mixed sediments	1.6	6.2
	Cobble/gravel	1.7	6.5
Rock bottom	Boulder/rubble	0.2	0.6
	Bedrock	7.0	26.7

Table 5. Substrate distribution by depth zone for the West Arm.

CMECS Subclass	Shallow infralittoral: 0–5 m water depth		Deep infralittoral: 5–30 m water depth		Circalittoral: 30–80 m water depth		Circalittoral (offshore): 80–200 m water depth		Mesobenthic: 200–1,000 m water depth	
	Percent	Area (km^2)	Percent	Area (km^2)	Percent	Area (km^2)	Percent	Area (km^2)	Percent	Area (km^2)
Unclassified soft-bottom	0.3	1	3.9	15	4.1	15.9	3.4	13.1	2.6	10
Mud	0	0	2.1	8.1	9.3	35.8	17.5	67.3	43	165.2
Sand	0	0.1	0.5	2	0.7	2.8	1.0	3.9	0.7	2.9
Mixed	0	0	0.2	0.8	0.4	1.6	0.7	2.5	0.3	1.2
Cobble/ gravel	0.1	0.3	0.5	1.9	0.2	0.8	0.3	1.1	0.6	2.4
Boulder/ rubble	0	0	0	0.1	0.1	0.3	0.0	0.2	0	0
Bedrock	0	0	0.4	1.7	1.3	4.9	2.4	9.2	2.8	10.7

environment, variation may be seasonal, reflecting changes in stream discharge and sea-ice cover. In the latter, temporal variation is likely less predictable with predominately hemipelagic sedimentation punctuated by infrequent and perhaps catastrophic gravity flows and rock falls. Sand and cobble/gravel subclasses are predominately associated with the delta and fan geoforms, most commonly found in shallow nearshore environments. The primary exception occurs along submarine channels where sand may be transported into the distal areas of the basin.

Geoform Component

The West Arm lies within the continental margin megageoform and is also a fjord megageoform. For simplicity, we characterized geoforms down to the mesogeoform scale (tens of meters to kilometers in size). Additionally, the resolution of our data was a limiting factor in geoform characterization. The primary mesogeoforms characterized within the West Arm are fjord wall/rock outcrop, floor, delta /fan, and moraine geoforms. Minor geoforms include slumps and submarine channels (table 6). The high relative proportion of walls, floors, and moraines is expected and is characteristic of glacial fjord

Table 6. Major geoform distribution for the West Arm.

Megageoform	Mesogeoform	Percentage of total area	Area (km²)
Fjord	Channel	1.8	6.8
	Delta/Fan	7.1	27.3
	Floor	33.9	130.4
	Moraine	29.3	112.5
	Slump	0.2	1.0
	Wall/Rock Outcrop	27.6	106.2

morphology. Numerous deltas exist along the fjord walls that are both fluvial and glacifluvial in origin, with most at least partially fed by glacial meltwater.

While certain geoforms are inherently related to specific substrates (for example, the floor geoform and the mud substrate), such associations should be made with caution. For example, rock drumlins in Scidmore Bay (fig. 6) are classified with the wall/rock outcrop class, implying that the morphology of the feature is bedrock controlled. The surficial sediment, however, consists of a heterogeneous mixture of bedrock, gravel, sand, and mud. Similarly many areas classified as moraine within the West Arm are partially or entirely draped in mud. In a dynamic environment, geoforms are the product of both relict and modern processes. Drawing direct associations between habitat and geoform should be done on a case-by-case basis, accounting for local conditions.

Large areas in the vicinity of Hugh Miller Inlet are characterized as moraine using CMECS terminology (sheet 3). These features are associated with an interval of quasi-stability and downwasting coeval to rapid retreat in the deeper West Arm proper. Upfjord, three prominent transverse ridges are also labeled as "moraines" (sheet 4). These bathymetric highs are inferred to be morainal banks composed primarily of coarse ice-contact material deposited during the retreat of Russell System. The mid-1870s and 1892 terminus positions correlate to the moraines south of Reid Inlet and at the mouths of Tarr and Johns Hopkins inlets, respectively. Within Johns Hopkins Inlet, a smaller, partially buried morainal bank, deposited around 1912, is still distinguishable across the inlet where it bends to the southwest. Seismic data reveal acoustic transparency at depth in some of these features, suggesting they are bedrock-cored and therefore sills, whereas others appear to be composed of purely discontinuous, hummocky, and mounded reflections interpreted to be ice-contact material (Cai, 1994). Consequently, the overall size of the feature is both a product of relict topography and the length of the interval of deposition. Extensive areas of the fjord walls are also characterized as moraine, which include remnants of kame terraces and partially buried terminal moraines. From an ecological perspective, these morainal forms can provide diverse habitats in relatively shallow water, as in Hugh Miller Inlet and near the mouth of Tidal Inlet. Deeper morainal deposits (below 80 m water depth) are typically buried under the hemipelagic drape that dominates the deeper basins.

The results of this study suggest that geoform, as inferred from bathymetric data, may not be an effective predictor of substrate in the active fjord environment. Consideration must also be paid to bathymetric position, water depth, and potential for sediment transport and removal, along with the influence of relict bathymetry. Within the West Arm, the only geoform that proved to be an accurate indicator of substrate was the fjord floor, which was 99 percent mud and most commonly associated with the mesobenthic depth zone (table 7, 8). This is not surprising, considering most of the hemipelagic sediment deposited within the fjord is eventually redistributed to the fjord floor basins, and few processes are capable of transporting abundant course material into the deep distal portions of the fjord. Substrate associations with other geoforms were more tenuous and are subject to the considerations enumerated above. Deltas, typically associated with sandy substrate, commonly have coarser topsets. Additionally the high influx of glacially sourced fines in the upper inlets can effectively bury active foresets in mud. Similarly, areas classified as wall are covered in a diversity of substrate types, but most commonly mud or unclassified unconsolidated sediment. Even steeply sloping bedrock outcrops were found to have significant mud cover.

The geoform component is particularly useful in the West Arm for assessing areas of potential change. Large and rapid remobilization of sedimentary landforms has been observed in Glacier Bay (Hunter, 1994). Further, Glacier Bay is located in a seismically active region, because of its proximity to the Queen Charlotte-Fairweather Fault. In the event of a significant earthquake, the potential is high for catastrophic slope failures from fjord walls. Deltaic complexes are particularly susceptible to failure, because of their unconsolidated composition and position resting on very steep bedrock. Such a failure would result in widespread sediment redistribution into the deep basin areas, burying any marine life in its proximity. Activation of submarine landslides by wave activity is unlikely, however, as waves in the fjord are fetch-limited. There is also potential for landslide-induced wave activity, although the magnitude and severity of these events is unknown.

Table 7. Percent mud cover versus geoform for the West Arm.

CMECS mesogeoform	Mud cover	
	Area (km^2)	Percent
Moraine	89.5	79.6
Wall[1]	37.5	35.0
Floor	129.2	99.1

[1] An additional 33.35 percent of wall forms are suspected of having unconsolidated sediment cover, most likely dominated by mud.

Table 8. Major geoform distribution by depth zone for the West Arm.

CMECS Class	Shallow infralittoral: 0–5 m water depth		Deep infralittoral: 5–30 m water depth		Circalittoral: 30–80 m water depth		Circalittoral (offshore): 80–200 m water depth		Mesobenthic: 200–1,000 m water depth	
	Percent	Area (km^2)	Percent	Area (km^2)	Percent	Area (km^2)	Percent	Area (km^2)	Percent	Area (km^2)
Channel	0	0	0		0	0	0.77	2.9	1.02	3.9
Delta/fan	0.08	0.3	0.59	2.3	1.26	4.8	1.7	6.5	3.47	13.3
Floor	0	0	0.58	2.2	3.69	14.2	6.08	23.4	23.58	90.6
Moraine	0.16	0.6	3.27	12.6	4.35	16.7	8.77	33.7	13.3	51.1
Slump	0	0	0.04	0.1	0.05	0.2	0.14	0.5	0.04	0.2
Wall	0.19	0.7	4.04	15.5	6.81	26.2	7.92	30.4	8.69	33.4

Water Column Component

Water column interpretations in this study are derived from those presented in Trusel and others (2010) and Etherington and others (2007a). Similar to the benthic cover and geoform components, the water column component is classified within the estuarine system. Benthic depth zones associated with oceanographic stations in the West Arm are classified as circalittoral offshore (80–200 m) and mesobenthic (200–1,000 m). The upper water column within the West Arm (above the pycnocline) is always in the epipelagic water column depth zone (>0–200 m), while the lower water column varies between epipelagic and mesopelagic (200–1,000 m).

Despite the fact that there is large spatial heterogeneity in tidal range within Glacier Bay (Hill, 2007), all stations in Glacier Bay, including those in the West Arm, were classified by CMECS as moderate tide range (1–5 m). Similarly, although there is large spatial heterogeneity in tidal velocity throughout Glacier Bay, including regions of extreme tidal currents (Hill, 2007; Hill and others, 2009), the use of averages within the CMECS system defined energy intensity within the upper water column at all stations as low energy (very weak currents; 0–2 knots). For all stations in the West Arm except stations 6 and 7, the upper layer energy type is classified as current (due to freshwater discharge and down-Bay flow), while the bottom water column energy type is considered to be tide. Station 6 and 7 are more mixed and are influenced by tidal energy in both the upper and lower water layers. Energy direction in the upper water layers of the West Arm as well as the rest of Glacier Bay is considered horizontal.

Upper and lower water column temperatures in the West Arm were classified as cold (0–10°C). Across all the West Arm stations, bottom waters were classified as euhaline (30–40 psu). Upper water layers within the West Arm were mostly classified as mesohaline (5–18 psu), whereas the most seaward of the stations within the West Arm (station 6) was classified as polyhaline (18–30 psu). The averaging of salinity to obtain a single classification measurement removed the large seasonal variation in salinity patterns in the West Arm (see Etherington and others, 2007a). For all stations in the West Arm except station 6, the primary water source for the upper water layers is watershed due to the influence of freshwater discharge from glacier, snow, and groundwater sources, while the bottom layers are primarily influenced by local estuary exchange (tidal exchange that is primarily estuarine water). For station 6, the primary water source for both the upper and bottom water layers is local estuary exchange due to the more seaward location, shallower depth, and resultant higher mixing.

Macrohydroforms and mesohydroforms as defined by CMECS were not identified for Glacier Bay. The only identifiable CMECS lifeform was the phytoplankton maximum layer, which was assigned to the upper water layer for all oceanographic stations. Trophic status (defined as general categorization of the abundance of dissolved macronutrients (DIN and DIP) and level of primary productivity of a unit; Madden and others, 2008) is considered oligotrophic (<5 µg/L chlorophyll *a)* for both upper and lower water layers at all stations within Glacier Bay when averages are calculated over the whole year. No water column biotopes were identified.

Despite the highly variable nature of the water-column environment, particularly within an estuarine fjord system, the CMECS system provides only one opportunity to incorporate temporal variability (for all classes and attributes combined) into the classification of the water column. For all of Glacier Bay, the upper water column was classified with a temporal persistence value of variable (varies regularly), while the persistence of the bottom water layers was considered permanent (stable). It was not possible to identify multiple sources of variation (for example, seasonal plus stochastic), so the dominant source of temporal change (seasonal) was defined.

Using the CMECS classification system, the water column properties that illustrated the greatest amount of spatial variation in Glacier Bay, horizontally (among stations) and (or) vertically (between the upper and lower water layers), include benthic depth, salinity, energy source, and primary water source (fig. 7). Upper water layers demonstrate greater complexity than the bottom water layers, with a greater number of unique combinations of classes (habitat units) in the upper layer. There were only two bottom water layer habitat units in the West Arm that vary only in benthic depth zone, with station 21 exhibiting shallower depth than the rest of the West Arm (fig. 7*A*). Within the West Arm, there were four different habitat units of the upper water layer that varied by benthic depth, salinity, energy type, and primary water source (fig. 7*B*). The majority of the upper water column within the West Arm is composed of mesohaline waters that are mainly influenced by watershed sources and current energy within mesobenthic depths. Upper water layers of station 21 differ from the mainstem waters of the West Arm only in the benthic depth zone (circalittoral offshore). The upper water column habitats of station 6 differ from the other West Arm stations more substantially, with different classes of salinity, energy type, and primary water source that reflect its more seaward location.

Sediment Accumulation

Average annual sediment accumulation rates for the period 1970 or 1972 to 2009 are shown in 8. Some basin-floor areas within the West Arm have no accumulation or even slight erosion (fig. 8: ~ 0 m/yr). Lacking evidence of strong currents, such areas are thought to be beyond the resolution of our data and are inferred to receive a low debris flux similar to the surrounding benthic environment.

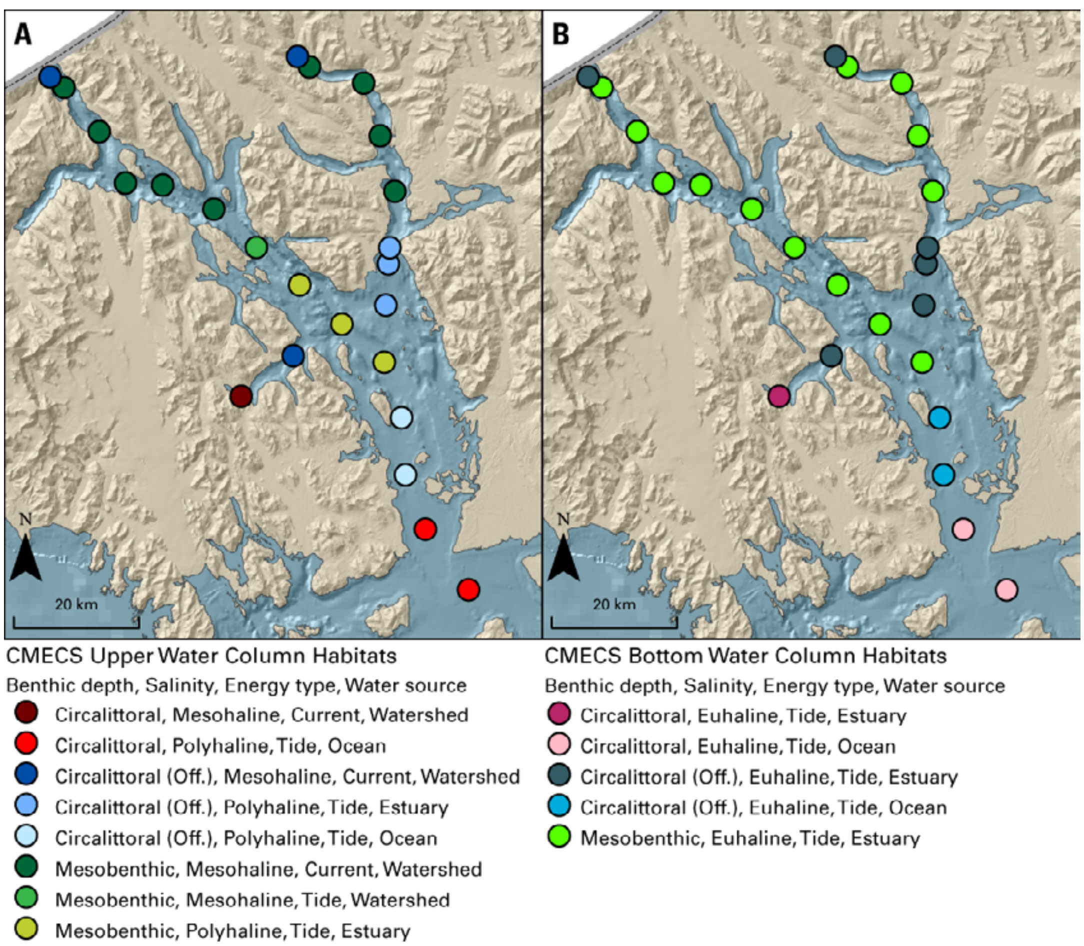

Figure 7. Maps of (*A*) upper and (*B*) bottom water column CMECS habitats in Glacier Bay areas (Trusel and others, 2010)

The West Arm can be divided into two modern sedimentation regimes: glacial sedimentation in the upper ice-contact basins of Tarr and Johns Hopkins Inlets and a marine paraglacial sedimentation regime that exists in all basins in the lower West Arm. Measured rates in the upper basins average 0.6 m/yr, whereas in the lower basins sediment accumulation rates are far less, averaging 0.1 m/yr. If the influence

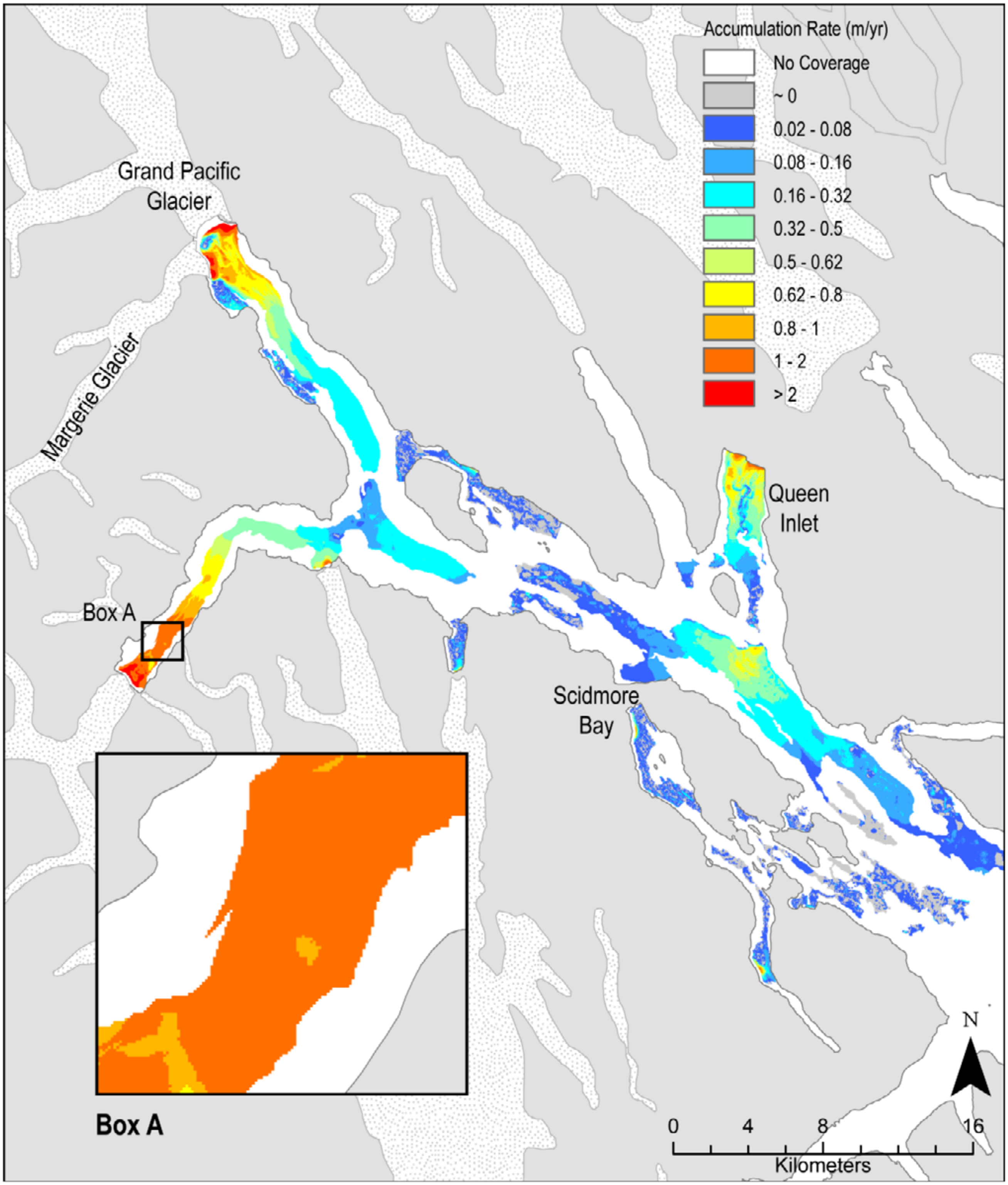

Figure 8. Map of average annual sediment accumulation rates for 1970 and 1972 to 2009.

of Queen Inlet is excluded, average sedimentation rates for the lower West Arm approach 0 m/yr yet are still sufficient to drape the seascape in glacimarine mud. The West Arm can be split into two primary physical benthic environments. The upper West Arm receives significant sediment flux, increasing the likelihood of gravity flows along the steep fjord walls, morainal banks, and ice-contact deltas. Terrestrially-sourced rock falls and debris flows are also more prevalent, owing to the steep relief of the fjord walls and limited vegetation cover associated with recent glacial retreat. Conversely, the lower West Arm is characterized by a more static benthic environment with a lower potential for unconsolidated slope failures. Notable exceptions to this general rule are found in Queen and Tidal Inlets. Fed by nearby Carroll Glacier, the relatively high sediment flux into Queen Inlet is anomalous within the lower West Arm, creating a physical benthic environment that is inferred to be intermediate to those that typify the upper and lower West Arms. Sedimentation rates in the vicinity of Queen Inlet average 0.4 m/yr, with the bulk sediment accumulating near the fjord-head delta and the submarine fan at the mouth of the inlet. Due to data quality issues in the historical bathymetry, Tidal Inlet was excluded from the differential bathymetric analysis presented in this study. However, numerous slide and slump-like features are evident in the modern bathymetry (sheet 3: slump mesogeoform), suggesting that the benthic environment within Tidal Inlet is relatively dynamic compared to the mainstem of the West Arm. While the frequency of such events is unknown, they potentially pose a significant disturbance to the benthic communities along the fjord wall.

Sediment accumulation decay downfjord is not only a function of distance from the glacial termini but is also influenced by submarine landforms. Sedimentation decreases abruptly south of the morainal bank at the mouth of Tarr Inlet (sheet 4: moraine mesogeoform). Historically, this bank has acted as a dam to the downfjord transport of sediment via bottom currents, confining the majority of sediment originating from Margerie and Grand Pacific Glaciers within Tarr Inlet (Cai, 1994). However, the 2009 bathymetry indicates the morainal bank may have reached its capacity as a sediment trap. If this is the case, sediment may begin to bypass Tarr basin, forming a fan at the mouth of the inlet. There are already signs of slope failure and possibly incision along the West end of the fjord-mouth morainal bank, evident in the 2009 bathymetry. This knickpoint may eventually propagate upfjord, creating a direct pathway for sediment transport into the mainstem of the West Arm. Eventually the spatial pattern of sedimentation in Tarr Inlet may take a form similar to that observed in Queen Inlet, with two main loci of deposition: one at the fjord head and another at a fjord mouth fan. Whether or not this occurs and to what extent depends on the composition of the morainal bank. Seismic reflection profiles indicate the bank may be primarily bedrock cored with a thin veneer of unconsolidated sediment (Cai, 1994), restricting submarine incision. If, however, the sill only extends across a portion of the fjord mouth, as in neighboring Johns Hopkins Inlet, incision and slope failures could potentially excavate the unconsolidated portion of the morainal bank. The most recent bathymetry does not provide a conclusive answer, but it tends to support the latter scenario (fig. 9).

Sediment accumulation occurring in the most proximal basin has ramifications for local benthic life, because of the pronounced sediment flux but also for glacier dynamics. Grounding-line deposits act as a second-order control on the stability of glacier termini (Powell, 1991; Fischer and Powell, 1998), and the development of an efficient pathway for sediment transport away from the grounding line could reduce terminus stability.

Benthic Habitats

Previous research has demonstrated classes of three bottom types most important to benthic organisms: soft-flat bottom, mixed bottom including coarse sediment and low-relief rock with low to moderate rugosity, and rugose-hard bottom (Greene and others, 2007; Cochrane, 2008). The West Arm has all of these of habitats, with the greatest abundance being soft-flat bottom. In Glacier Bay, species

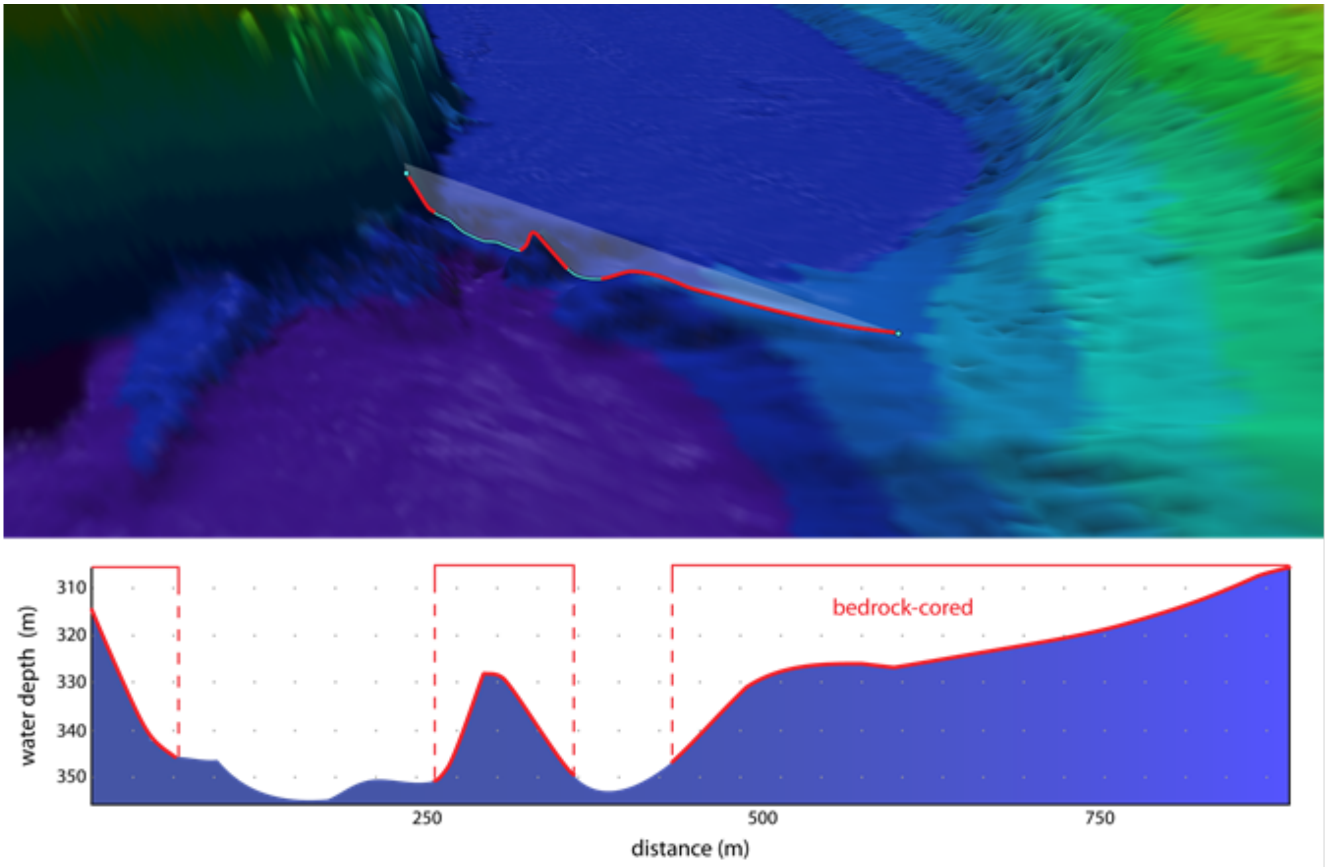

Figure 9. Perspective view and cross section of the morainal bank at the mouth of Tarr Inlet.

associated with soft-flat bottom habitats include gastropods, algae, flatfish, Tanner crabs, shrimp, sea pen, and other crustaceans (Etherington and others, 2007b). In the bay proper, soft corals and sponge are the only species found associated with boulder substrate (Etherington and others, 2007b). Our video observations suggest that geological-biological associations found in central Glacier Bay to be at least partially analogous to associations in the West Arm. Given that soft mud substrate is the most prevalent habitat in the West Arm, it is expected that the species associated with a soft bottom in the bay proper are the most abundant types of species within the West Arm. While mud is the dominant substrate throughout the fjord, the upper and lower West Arm are potentially very different environments owing to the spatially and temporally heterogeneous influence of glaciation and associated effects on fjord hydrologic and oceanographic conditions. Therefore, we expect variations in the distribution of species accordingly.

The distribution of Tanner crab (*Chionoecetes bairdi*), a mud-associated species, may be a potential example of the two contrasting environments. Systematic sampling shows that Tanner crabs are found throughout the West Arm but are generally most abundant near fjord-mouth sills and sparse in the ice-contact inlets and the deeper fjord basins (Mondragon and others, 2007a; Nielsen and others, 2007). Juvenile females were very dense in Scidmore-Charpentier Inlet, which is hypothesized to represent a suitable habitat for juveniles as opposed to adults, because of the generally lower biomass and food resources associated with glacial proximity (Nielsen and others, 2007). Relative to the upper West Arm, however, Scidmore-Charpentier receives a much lower glacial debris flux. Indeed, the upper

West Arm is likely a much harsher environment because of the extreme glacial influence and associated characteristics. The higher sediment flux may explain why juvenile Tanner crabs were not abundant in the similar soft bottom habitat near the upper West Arm glaciers.

The West Arm has both shallow- and deep-water benthic habitats. However, unlike Glacier Bay proper where large contrasts in the depth and current velocity define habitats (Etherington and others, 2007b), current velocities are relatively low for most of the West Arm (Etherington and others, 2007a; Hill, 2007). Therefore, while substrate and current exposure are the dominant factors controlling species distribution in the Bay proper (Etherington and others, 2007b), currents are not as likely to play as large of a role in the West Arm. We expect substrate type and glacial proximity to be the most important habitat variables in the West Arm, although further groundtruthing is necessary to fully evaluate this hypothesis.

Conclusions

Seafloor substrates and morphology in the West Arm were mapped using a combination of data sources including multibeam bathymetry, video observations, backscatter data, and knowledge of the glacimarine environment. Substrate characterization, combined with information about depth, morphology, glacial influence, and current velocity provide the necessary variables to define potential benthic habitats in the West Arm. Mud is the dominant substrate within the West Arm, covering nearly 72 percent of the seafloor. Bedrock was the next most abundant substrate, covering about 7 percent of the surveyed area. The remaining portion of the West Arm is covered by a mixture of coarser sediment and boulder/rubble. We expect organisms found associated with similar habitats in the bay proper are also abundant in the West Arm, with the largest benthic communities being those associated with mud substrate.

The bulk of sediment flux from Johns Hopkins, Margerie, and Grand Pacific Glaciers is confined to the Upper West Arm basins. Because of the contrast in sediment accumulation rates between the upper and lower West Arm, the fjord can be characterized as two distinct regions—the dynamic Upper West Arm characterized by an extremely high glacial sediment flux and the relatively static Lower West Arm. The exceptions are the vicinity of Queen Inlet, which receives abundant sediment from Carroll Glacier, and Tidal Inlet, which is prone to mass wasting due to its steep, poorly consolidated valley walls. The benthic environments typical of the Lower West Arm can be further subdivided into the mesobenthic basin constrained to the West Arm proper and the predominately circalittoral bays and inlets.

Glacial meltwater and debris flux are known to affect the spatial distribution and variety of benthic fauna and flora in the arctic (for example, Wlodarska-Kowalczuk and Pearson, 2004) and to control the distribution and diversity of wall communities in Tarr Inlet, in spite of adequate nutrient supply (Carney and others, 1999). However, the degree to which these variables act as physical controls in the deep basins is unknown. The temperate glacimarine environment, with some of the highest sediment fluxes recorded worldwide, may limit the diversity, abundance, and distribution of these benthic communities, particularly in upper Tarr and Johns Hopkins Inlets where sediment flux is pronounced. Likewise, there exists the potential for areas of intermediate disturbance along the fjord axis that likely support higher diversity and abundance. Further study of the seafloor environment in the upper fjords is critical for a more quantitative evaluation of these relations. However, the extreme turbidity of the water column in the ice-proximal portions of these basins may limit the effectiveness of video observation.

Management Implications

This work presents the first surficial geology and geoform maps for the West Arm of Glacier Bay. Substrate, morphology, depth, water column, and glacial processes are all important factors in determining the distribution, abundance, and diversity of demersal and benthic marine life. Therefore, these products are important to scientists and managers to better understand the capacity of the West Arm to act as a marine reserve. These results are a baseline for the assessment of future environmental change, resulting from the influences of proximal glaciation, as well as dynamic fjord processes. With stresses on the glacial estuary because of amplified high-latitude climate change and the commercial, recreational, and scientific importance of the Glacier Bay ecosystem, a full understanding of the modern system is fundamental for understanding its resources and developing the most appropriate management strategies.

Acknowledgments

Funding for this benthic habitat study was provided by the National Park Service. The authors would like to thank Luke Trusel for providing the boilerplate of his habitat study in Muir Inlet. Special thanks to the captain and crew of R/V *Steller*, as well as Gerry Hatcher and Jamie Grover of USGS for their efforts in our field operations. Assistance from Nadine Golden with USGS mapping standards is greatly appreciated.

References Cited

Anderson, T.J., Cochrane, G.R., Roberts, D.A., Chezar, H., and Hatcher, G., 2008, A systematic real-time method to characterize seafloor habitats and benthic macro-organisms—Habitat mapping with a side-scan sonar and towed camera-sled: Mapping the Seafloor for Habitat Characterization, Geological Association of Canada, Special Paper 47, p. 71–79.

Cai, J., 1994, Sediment yields, lithofacies architecture, and mudrock characteristics in glacimarine environments: DeKalb, Northern Illinois University, unpublished Ph.D. dissertation.

Cai, J., Powell, R.D., Cowan, E.A., and Carlson, P.R., 1997, Lithofacies and seismic reflection interpretations of temperate glacimarine sedimentation in Tarr Inlet, Glacier Bay, Alaska: Marine Geology, v. 145, p. 5–37.

Carlson, P.R, Cowan, E.A., Powell, R.D., Cai, J., 1999, Growth of a post-Little Ice Age submarine fan, Glacier Bay, Alaska: Geo-Marine Letters, v. 19, p. 227–239.

Carlson, P.R., Hooge, P., Cochrane. G., Stevenson, A., Dartnell, P., and Lee, K., 2002, Multibeam bathymetry and selected perspective views of main part of Glacier Bay, Alaska: U.S. Geological Survey Open-File Report 02–391, *http://geopubs.wr.usgs.gov/open-file/of02-391/*.

Carney, D., Oliver, J.S., and Armstrong, C., 1999, Sedimentation and composition of wall communities in Alaskan fjords: Polar Biology, v. 22, p. 39–49.

Cochrane, G.R., 2008, Video-supervised classification of sonar data for mapping seafloor habitat, *in* Reynolds, J.R., and Greene, H.G., eds., Marine habitat mapping technology for Alaska: University of Alaska Fairbanks, Alaska Sea Grant College Program, p. 185–194.

Cowan, E.A., and Powell, R.D., 1990, Suspended sediment transport and deposition of cyclically interlaminated sediment in a temperate glacial fjord, Alaska, U.S.A., *in* Dowdeswell, J.A., and Scourse, J.D., eds., Glacimarine environments—Processes and sediments: Geological Society Special Publication 53, p. 75–89.

Cowan, E.A., and Powell, R.D., 2007, High frequency climate signals in fjord sediments of Glacier Bay National Park Alaska, *in* Piatt, J.F., and Gende, S.M., eds., Proceedings of the Fourth Glacier Bay Science Symposium, October 26–28, 2004: U.S. Geological Survey Scientific Investigations Report 2007–5047, p. 46–49.

Cowan, E.A., Powell, R.D., Carlson, P.R., Kayen, R.E., Cai, J., Seramur, K.C., Zellers, S.D., 1994, Cruise report—R/V *Alpha Helix* Cruise-173 to western Prince William Sound, Yakutat Bay, and Glacier Bay National Park, southeastern Gulf of Alaska, August 17–September 3, 1993: U.S. Geological Survey Open-File Report 94–258, 181 p.

Cowan, E.A., Seramur, K.C., Cai, J., and Powell, R.D., 1999, Cyclic sedimentation produced by fluctuations in meltwater discharge, tides, and marine productivity in an Alaskan fjord: Sedimentology, v. 46, p. 1109–1126.

Elverhøi, A., Hooke, R. LeB., and Solheim, A., 1998, Late Cenozoic erosion and sediment yield from the Svalbard-Barents Sea Region—Implications for understanding erosion of glacierized basins: Quaternary Science Reviews, v. 17, p. 209–241.

Environmental Systems Research Institute (ESRI), 2005, ArcGIS 9.2 computer software: Redlands, California, Environmental Systems Research Institute, Inc.

Etherington, L., Cochrane, G., Harney, J., Taggart, J., Mondragon, J., Andrews, A., Madison, E., Chezar, H., and de La Bruere, J., 2007b, Glacier Bay seafloor habitat mapping and classification—First look at linkages with biological patterns, *in* Piatt, J.F., and Gende, S.M., eds., Proceedings of the Fourth Glacier Bay Science Symposium, October 26–28, 2004: U.S. Geological Survey Scientific Investigations Report 2007–5047, p. 71–75.

Etherington, L.L., Hooge, P.N., Hooge, E.R., and Hill, D.F., 2007a, Oceanography of Glacier Bay, Alaska—Implications for biological patterns in a glacial fjord estuary: Estuaries and Coasts, v. 30, no. 6, p. 927–944.

Fischer, M.P., and Powell, R.D., 1998, A simple model for the influence of push-morainal banks on the calving and stability of glacial tidewater termini: Journal of Glaciology, v. 44, p. 31–41.

Goldwait, R.P., 1974, Rates of formation of glacial features in Glacier Bay, Alaska, *in* Coates, D.R., ed., Glacial geomorphology: Binghamton, State University of New York, v. 5, p. 163–185.

Greene, H.G., Bizzaro, J.J., O'Connell, V.M., and Brylinsky, C.K., 2007, Construction of digital potential marine benthic habitat maps using a coded classification scheme and its application, *in* Todd, B.J., and Greene, H.G., Mapping the seafloor for habitat characterization: Geological Association of Canada Special Paper 47, p. 141–155.

Greene, H.G., Yoklavich, M.M., Starr, R., O'Connell, V.M., Wakefield, W.W., Sullivan, D.L. MacRea, J.E., and Cailliet, G.M., 1999, A classification scheme for deep-water seafloor habitats: Oceanographica Acta, v. 22, no. 6, p. 663–678.

Hall, D.K., Benson, C.S., and Field, W.O., 1995, Changes of glaciers in Glacier Bay, Alaska, using ground and satellite measurements: Physical Geography, v. 16, no. 1, p. 27–41.

Hallet, B., Hunter, L., and Bogen, J., 1996, Rates of erosion and sediment evacuation by glaciers—A review of field data and their implications: Global and Planetary Change, v. 12, p. 213–235.

Harney, J.N., Cochrane, G.R., Etherington, L.L., Dartnell, P., Golden, N.E., and Chezar, H.. 2007, Geologic characteristics of benthic habitats in Glacier Bay, Alaska, derived from geophysical data, videography, and sediment sampling, *in* Piatt, J.F., and Gende, S.M., eds., Proceedings of the Fourth Glacier Bay Science Symposium, October 26–28, 2004: U.S. Geological Survey Scientific Investigations Report 2007–5047, p. 37–41.

Hill, D.F., 2007, Tidal modeling of Glacier Bay, Alaska—Methodology, results, and application: State College, Pennsylvania State University, unpublished report, 139 p., *http://water.engr.psu.edu/hill/research/glba/default.stm*.

Hill, D.F., Ciavola, S.J., Etherington, L., and Klaar, M.J., 2009, Estimation of freshwater runoff into Glacier Bay, Alaska, and incorporation into a tidal circulation model: Estuarine, Coastal, and Shelf Science, v. 82, p. 95–107, doi:10.1016/j.ecss.2008.12.019.

Hooge, P.N., and Hooge, E.R., 2002, Fjord oceanographic processes in Glacier Bay, Alaska: U.S. Geological Survey, Alaska Science Center, unpublished report to National Park Service, Glacier Bay National Park, 148 p.

Hunter, L.E., 1994, Grounding-line systems and glacier mass balance of modern temperate glaciers and their effect on glacier stability: DeKalb, Northern Illinois University, unpublished Ph.D. dissertation.

Hunter, L.E., Powell, R.D., and Lawson, D.E., 1996, Flux of debris transported by ice at three Alaskan tidewater glaciers: Journal of Glaciology, v. 42, p. 123–135.

Larson, C.F., Motyka, R.J., Echelmeyer, K.A., and Geissler, P.E., 2007, Glacier changes in southeast Alaska and northwest British Columbia and contribution to sea level rise: Journal of Geophysical Research, v. 112, p 1–11.

Larsen, C.F., Motyka, R.J., Freymueller, J.T., Echelmeyer, K.A., and Ivins, E.R., 2004, Rapid uplift of southern Alaska caused by recent ice loss: Geophysical Journal International, v. 158, p. 1118–1133.

Luthcke, S.B., Arendt, A.A., Rowlands, D.D., McCarthy, J.J., and Larsen, C.F., 2008, Recent glacier mass changes in the Gulf of Alaska region from GRACE mascon solutions: Journal of Glaciology, v. 54, no. 188, p. 767–777.

Madden, C.J., Goodin, K., Allee, R.J., Cicchetti, G., Moses, C., Finkbeiner, M., and Bamford, D., 2009, Draft Coastal and Marine Ecological Classification Standard: National Oceanic and Atmospheric Administration (NOAA) and NatureServe, v. III, 109 p.

Madden, C.J., Goodin, K.L., Allee, R., Finkbeiner, M., and Bamford, D.E., 2008, Draft Coastal and Marine Ecological Classification Standard: National Oceanic and Atmospheric Administration (NOAA) and NatureServe, v. III, 77 p.

Meier, M.F., Dyurgerov, M.B., Rick, U.K., O'Neel, S., Pfeffer, T., Anderson, R.S., Anderson, S.P., and Glazovsky, A.F., 2007, Glaciers dominate eustatic sea-level rise in the 21st century: Science, v. 317, no. 5841, p. 1064–1067.

Mondragon, J., Etherington, L., Taggart, S.J., Hooge, P.N. 2007b, The distribution and abundance of Pacific Halibut in a recently deglaciated fjord—Implications for marine reserve design, *in* Piatt, J.F., and Gende, S.M., eds., Proceedings of the Fourth Glacier Bay Science Symposium, October 26–28, 2004: U.S. Geological Survey Scientific Investigations Report 2007–5047, p. 107–109.

Mondragon, J., Taggart, S.J., Andrews, A.G., Nielsen, J.K., de La Bruere, J., 2007a, Spatial distribution and relative abundance of Tanner and red king crab inside and outside of marine reserves in Glacier Bay, Alaska, *in* Piatt, J.F., and Gende, S.M., eds., Proceedings of the Fourth Glacier Bay Science Symposium, October 26–28, 2004: U.S. Geological Survey Scientific Investigations Report 2007–5047, p. 84–86.

NGDC, 2012, Index to Marine & Lacustrine Geological Samples: National Oceanic & Atmospheric Administration (NOAA) National Geophysical Data Center, Boulder, Colo., *http://www.ngdc.noaa.gov/mgg/curator/curator.html*.

Nielsen, J.K., Taggart, S.J., Shirley, T.C., and Mondragon, J., 2007, Spatial distribution of juvenile and adult female Tanner crabs (*Chionoecetes bairdi*) in a glacial fjord ecosystem—Implications for recruitment processes: ICES Journal of Marine Science, v. 64, p. 1772–1784.

NOAA, 1970a, Descriptive Report, Hydrographic Survey H09138, vicinity of Composite Island, Alaska: Norfolk, VA, National Oceanic and Atmospheric Administration (NOAA) National Ocean Service, *http://surveys.ngdc.noaa.gov/mgg/NOS/coast/H08001-H10000/H09137/DR/H09137.pdf*.

NOAA, 1970b, Descriptive Report, Hydrographic Survey H09139, Tlingit Point to Tidal Inlet, Glacier Bay, Alaska: Norfolk, VA, National Oceanic and Atmospheric Administration (NOAA) National Ocean Service, *http://surveys.ngdc.noaa.gov/mgg/NOS/coast/H08001-H10000/H09138/DR/H09138.pdf*.

NOAA, 1970c, Descriptive Report, Hydrographic Survey H09141, Queen and Rendu Inlets, Alaska: Norfolk, VA, National Oceanic and Atmospheric Administration (NOAA) National Ocean Service, *http://surveys.ngdc.noaa.gov/mgg/NOS/coast/H08001-H10000/H09141/DR/H09141.pdf*.

NOAA, 1970d, Descriptive Report, Hydrographic Survey H09142, Scidmore Bay and vicinity, Glacier Bay, Alaska: Norfolk, VA, National Oceanic and Atmospheric Administration (NOAA) National Ocean Service, *http://surveys.ngdc.noaa.gov/mgg/NOS/coast/H08001-H10000/H09142/DR/H09142.pdf*.

NOAA, 1970e, Descriptive Report, Hydrographic Survey H09143, Charpentier Inlet, Glacier Bay, Alaska: Norfolk, VA, National Oceanic and Atmospheric Administration (NOAA) National Ocean Service, *http://surveys.ngdc.noaa.gov/mgg/NOS/coast/H08001-H10000/H09143/DR/H09143.pdf*.

NOAA, 1972a, Descriptive Report, Hydrographic Survey H09315, John Hopkins Inlet and vicinity, Alaska: Norfolk, VA, National Oceanic and Atmospheric Administration (NOAA) National Ocean Service, *http://surveys.ngdc.noaa.gov/mgg/NOS/coast/H08001-H10000/H09315/DR/H09315.pdf*.

NOAA, 1972b, Descriptive Report, Hydrographic Survey H09316, Tarr Inlet, Glacier Bay, Alaska: Norfolk, VA, National Oceanic and Atmospheric Administration (NOAA) National Ocean Service, *http://surveys.ngdc.noaa.gov/mgg/NOS/coast/H08001-H10000/H09316/DR/H09316.pdf*.

NOAA, 2009a, Descriptive Report, Hydrographic Survey H12140, Northern Glacier Bay, Alaska: Norfolk, VA, National Oceanic and Atmospheric Administration (NOAA) National Ocean Service, *ftp://ftp.ngdc.noaa.gov/pub/coast/H12001-H14000/H12141/DR/H12141.pdf*.

NOAA, 2009b, Descriptive Report, Hydrographic Survey H12141, Northern Glacier Bay, Alaska: Norfolk, VA, National Oceanic and Atmospheric Administration (NOAA) National Ocean Service.

NOAA, 2009c, Descriptive Report, Hydrographic Survey H12142, Northern Glacier Bay, Alaska: Norfolk, VA, National Oceanic and Atmospheric Administration (NOAA) National Ocean Service.

Piatt, J.F., and Gende, S.M., eds., 2007, Proceedings of the Fourth Glacier Bay Science Symposium: U.S. Geological Survey Scientific Investigations Report 2007–5047, 246 p.

Powell, R.D., 1984, Guide to glacial geology of Glacier Bay, southeastern Alaska—Glacial history, glacial sedimentology, glacial geomorphology, and glaciomarine sedimentation: Anchorage, Alaskan Geological Society, 85 p.

Powell, R.D., 1991, Grounding-line systems as second-order controls on fluctuations of tidewater termini of temperate glaciers—Glacial marine sedimentation, paleoclimatic significance: Geological Society of America Special Paper 261**,** p. 75–94.

Powell, R.D., and Molnia, B.F., 1989, Glacimarine sedimentary processes, facies and morphology of the south-southeast Alaska shelf and fjords, *in* Powell, R.D., and Elverhøi, A., eds., Modern glacimarine environments—Glacial and marine controls of modern lithofacies and biofacies: Marine Geology, v. 85, p. 359–390.

Seramur, K.C., Powell, R.D., and Carlson, P.R., 1997, Evaluation of conditions along the grounding line of temperate marine glaciers—An example from Muir Inlet, Glacier Bay, Alaska: Marine Geology, v. 140, p. 307–328.

Syvitski, J.P.M., 1989, On the deposition of sediment within glacier-influenced fjords—Oceanographic controls, *in* Powell, R.D., and Elverhøi, A., eds., Modern glacimarine environments—Glacial and marine controls of modern lithofacies and biofacies: Marine Geology, v. 85, p. 301–329.

Trusel, L.D., Cochrane, G.R., Etherington, L.L., Powell, R.D., Mayer, L.A., 2010, Marine benthic habitat mapping of Muir Inlet, Glacier Bay National Park and Preserve: U.S. Geological Survey Scientific Investigations Map 3122.

Umbach, M.J., 1976, Hydrographic manual (4th ed.): U.S. Department of Commerce, Coast and Geodetic Survey, 400 p., *http://www.thsoa.org/pdf/hm1976/hmall.pdf*.

Wilson, J.C., and Overland, J.E., 1987, Meteorology, *in* Hood, D.W., and Zimmerman, S.T., eds., The Gulf of Alaska: U.S. Department of Commerce National Oceanic and Atmospheric Administration, p. 31–54.

Wlodarska-Kowalczuk, M., and Pearson, T.H., 2004, Soft-bottom macrobenthic faunal associations and factors affecting species distributions in an Arctic glacial fjord (Kongsfjord, Spitsbergen): Polar Biology, v. 27, p. 155–167.